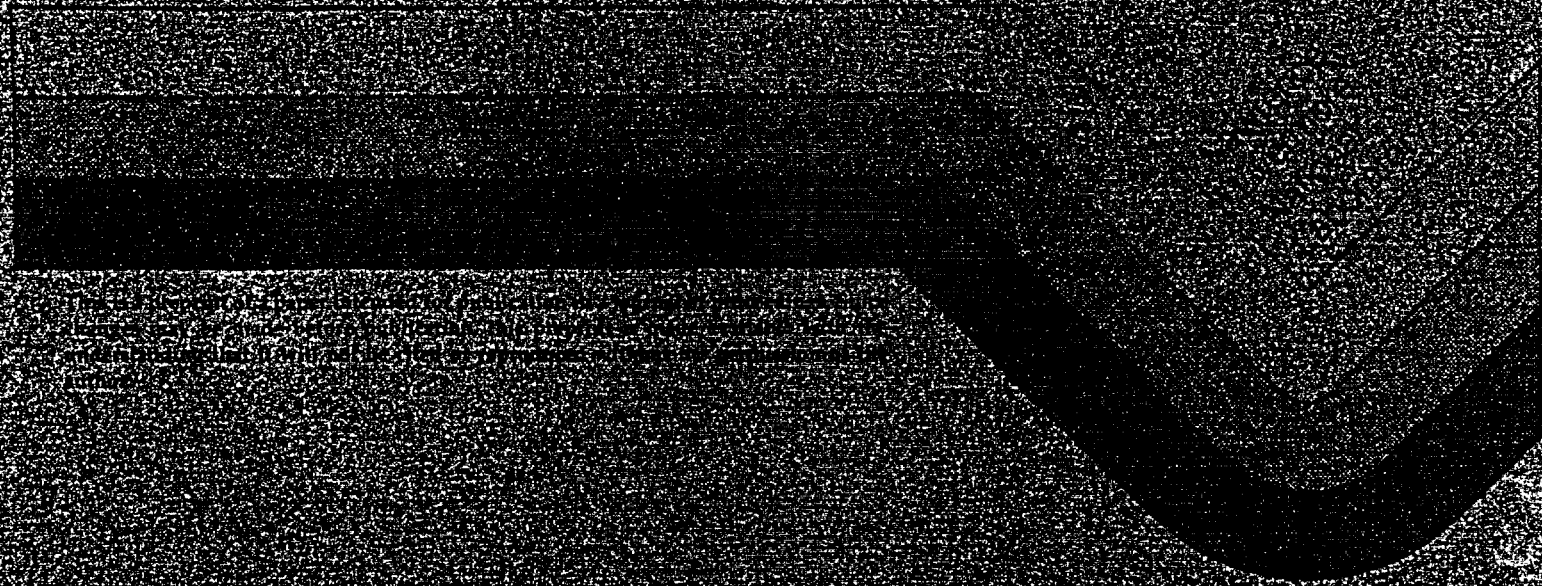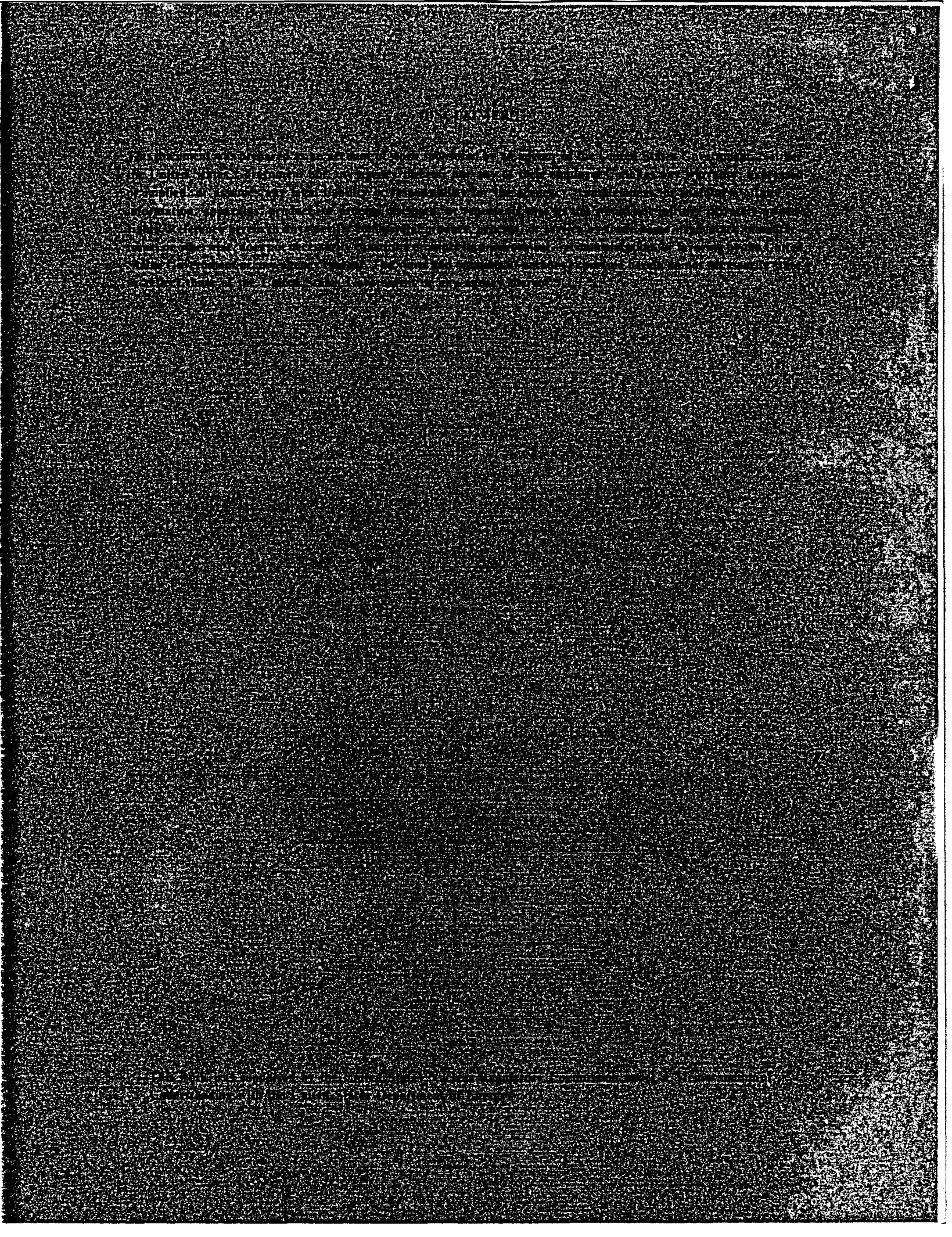# Chemical modeling of geologic disposal of nuclear waste: progress report and a perspective

T. J. Wolery

Manuscript date: September 1, 1980

LAWRENCE LIVERMORE LABORATORY
University of California • Livermore, California • 94550

CONTENTS

LIST OF FIGURES

ACKNOWLEDGMENTS

ABSTRACT

Chemical interactions among nuclear waste, groundwater, waste packaging, and rock are complex but critical factors in determining the consequences of geologic waste disposal. This report presents a perspective on the development of a theoretically based chemical modeling capability for application to nuclear waste geochemistry. It also presents some progress made in developing this capability.

The starting point in this study is the thermodynamic-arbitrary kinetics modeling developed by geochemists to study rock-water interactions. A number of other materials, including crystalline waste forms, packaging, buffers, and backfills, can be brought into this model by supplying appropriate thermodynamic data. In addition, other phenomena can, in principle, also be included in the model. These phenomena include realistic (nonarbitrary) kinetics, sorption, and radiolysis. Recent progress in the understanding both of mineral dissolution kinetics and of ionic substitutions in solid solution reported in the geochemical literature may strongly impact the state-of-the-art of modeling waste form, packaging, and chemical buffer performance in the geologic disposal of nuclear waste.

The performance of the EQ3/EQ6 software package for geochemical modeling has been improved, and its thermodynamic data base has been expanded to represent uranium and some other elements significant to waste disposal. Model calculations of UO_2 dissolution in granitic groundwaters confirm the importance of dissolved oxygen and of carbonate complexing of the uranyl ion in accounting for the magnitude of dissolved uranium in the temperature range 25 to 200 C. The maximum transient levels of dissolved uranium decrease with increasing temperature in this temperature range in response to the decreasing relative stabilities of the uranyl carbonate complexes. Simulations of UO_2 dissolution at 300 C based on thermodynamic extrapolations show higher levels of dissolved uranium. Speciation in these simulations is dominated by the complexes $UO_2SO_4^{o}$ and $UO_2(SO_4)_2^{2-}$.

Application to waste-container-groundwater interactions are illustrated by simulations of the codissolution of UO_2 and Cu metal in an oxidizing granitic groundwater at 100 and 300 C. Copper may partially protect UO_2 (in a chemical sense) by consuming dissolved oxygen. It is an attractive packaging component because it and groundwater may reach a state of thermodynamic equilibrium.

EXECUTIVE SUMMARY

This report focuses on the role of chemical modeling as a tool to predict the consequence of chemical interactions among nuclear waste forms, groundwater, packaging, rock, backfill, and engineered buffers. Such a modeling capability can be developed within a thermodynamic framework. However, it must also include provision for the significant nonequilibrium phenomena. These may include radioactive decay, radiolysis, and the kinetics of redox, sorption, dissolution, and precipitation reactions. Such a modeling approach may be taken for both far-field and near-field scenarios.

No such comprehensive model currently exists. Significant progress in developing such a modeling capability can be made within about three to five years; development of the full potential of the approach may take much longer. The logical starting point for creating such a modeling capability is the partial equilibrium-arbitrary kinetics model proposed by Helgeson (1968) for predicting the consequences of irreversible reaction in natural aqueous geochemical systems. Recent progress in understanding the dissolution of kinetics of mineral substances (reviewed in Chapter 3) and the thermodynamics of solid solutions (reviewed in Chapter 4) promises potentially rapid development in this aspect of the modeling, particularly with regard to predicting the long-term dissolution rates of crystalline waste forms such as spent fuel, supercalcine, and SYNROC.

Progress toward developing this modeling capability has been described in this report. This has dealt mainly with further development of a geochemical modeling code package (Wolery, 1979a), the expansion to date of its thermodynamic data base (principally the inclusion of data for aqueous species and solids of uranium), and the discussion of some arbitrary kinetic simulations of UO_2 dissolution and UO_2-Cu codissolution in plutonic groundwaters at temperatures ranging from 25 to 300 C. These simulations represent application of the modeling approach to waste-groundwater and waste-packaging-groundwater interactions.

Simulations at 25, 100, and 200 C show the strong dependence of dissolved uranium on the initial content of dissolved oxygen and carbonate of the groundwater. The aqueous speciation of uranium is dominated by the uranyl carbonate complexes, chiefly $UO_2(CO_3)_2^{2-}$, even under fairly reducing conditions. Codissolution of copper metal leads to the establishment of

copper-fluid equilibrium prior to UO_2-fluid equilibrium. Secondary copper metal may precipitate later in the overall reaction. Copper codissolution may reduce the level of dissolved uranium because Cu competes with UO_2 for available dissolved oxygen.

Simulations at 300 C, based on extrapolated thermodynamic data, predict different behavior. Levels of dissolved uranium may be significantly higher and show little dependence on dissolved carbonate. Under both oxidizing and fairly reducing conditions, most dissolved uranium is present as uranyl sulfate complexes (chiefly $UO_2SO_4^o$). Experimental confirmation of these predictions is in order.

Further development of this modeling approach requires work in several areas. One of these is continued expansion of the thermodynamic data base. Another is the development of data bases for both kinetics and the thermodynamics of solid solutions. Code development is also needed to include provision for phenomena not currently accounted for, such as radiolysis, chemical kinetic processes, realistic solid solution, and sorption. Computerized sorption models are already being developed in conjunction with thermodynamic equilibrium codes (cf. James and MacNaughton, 1977; Davis et al., 1978; Westall and Hohl, 1980) and the best or simplest of these should also be incorporated into irreversible reaction modeling software. Progress in chemical modeling requires basic theoretical and experimental research. However, the fundamental research required for understanding waste isolation problems should in large part be identified by empirical and field studies.

The model proposed here is by itself incomplete in the sense that it has no internal space coordinates. This may suffice to describe some experimental systems. More generally, nowever, it may be applied to describe the state of certain compartments of a larger model. Such a grand model in turn might govern the transfer of mass and heat among the various compartments over given intervals of time. Where small-scale diffusion processes are significant, such as glass alteration at low temperature, some compartments of the grand model might contain internal space coordinates. For example, such compartments might be represented by computerized versions of the glass alteration models of Hench et al. (1979).

Chapter 1

INTRODUCTION

Assessing the consequences of geologic disposal of nuclear waste requires capabilities to predict the complex chemical interactions that may occur in the near-field and far-field environments of a repository. Near-field interactions control the release of radionuclides to the surrounding hydrogeologic environment. They may be more difficult to model than far-field interactions due to high temperature gradients, radiolytic phenomena, and high concentration of chemically reactive substances.

Historically, model development for the near-field zone has taken a mostly fundamental approach, while that for the far-field has emphasized a phenomenological approach (Burkholder, 1979). This report is concerned with a fundamental approach to chemical modeling that may be applied to either the near-field or the far-field. Its purpose is twofold. First, it discusses a perspective on the current state-of-the-art in chemical modeling and how it can be further developed to meet the needs of programs for geologic disposal of nuclear waste. In particular, we briefly review recently developed work on the dissolution kinetics of mineral substances that may significantly impact chemical modeling in the near future. Application of the site-mixing concept to the thermodynamics of solid solutions appears to be an equally useful development in extending the power of chemical modeling.

The second purpose of this report is to present recent work conducted at this Laboratory toward developing an improved chemical modeling capability for application to waste isolation problems. This work includes further improvement to the EQ3/EQ6 software package (Wolery, 1979a), which simulates irreversible (nonequilibrium) reaction in aqueous systems following the approach originally laid down by Helgeson (1968) for modeling processes of rock-water interaction. We have expanded the thermochemical data base of the package to include aqueous and solid species of uranium, taking most of the new data from Langmuir's (1978) critically reviewed compilation. We then undertook a theoretical study of the consequences of irreversible dissolution of UO_2 in plutonic (granitic) groundwaters with and without a copper packaging component.

Chapter 2

THERMODYNAMIC-KINETIC MODELING
OF WASTE INTERACTIONS

2.1 PERSPECTIVE

The approach of this work is to develop an understanding of near-field
interactions within the framework of thermodynamics. The most widely
recognized branch of thermodynamics is _equilibrium_ thermodynamics. It
provides much of the theoretical structure of physical chemistry. Its
principles have been extensively applied in modeling the geochemistry of
aqueous systems (Garrels and Christ, 1965; Krauskopf, 1967; Stumm and Morgan,
1970; Berner, 1971). Computer codes have been developed to generate
equilibrium models. Most of these codes have been reviewed by Nordstrom et
al. (1979).

Models that include provisions for treating a set of reactions not in a
state of equilibrium are also required to assess the consequences of geologic
disposal of nuclear waste. Helgeson (1968) and Helgeson et al. (1970)
developed a model for _irreversible_ (nonequilibrium) reaction between minerals
and aqueous solutions in which fixed relative rates of dissolution of a set of
reacting minerals are assumed to be rate limiting on the system as a whole.
Other reactions, such as precipitation and dissolution of secondary minerals
and reactions occurring only among aqueous species (i.e., ion-pairing,
complexing, and homogeneous redox coupling), were assumed to adjust to the
former dissolution reactions so as to be in states of equilibrium at any
instant in the overall process.

This model, though idealized, has been successfully applied to
understanding rock-water interactions in a variety of geologic settings
(Helgeson et al., 1969; Apps et al., 1978). It is a basis for developing a
more realistic model that may be applied to systems and scenarios where some
of the above assumptions do not hold. For example, recent developments in the
theory of mineral dissolution (Chapter 5) promise to permit proper treatment
of irreversible dissolution rates; consequently, the modeler may soon be
constrained no longer by having to choose arbitrary, constant rate values.

Thermodynamic models (equilibrium or irreversible) are generally applied to systems that do not require internal space coordinates in their description. Temperature, pressure, and the chemical potentials of the thermodynamic components are uniform over the volume of the model systems; each phase, therefore, has a uniform composition. A kinetic model can be directly superimposed on such a thermodynamic model if it deals only with true reaction kinetics and not transport phenomena (i.e., diffusion, because the description of concentration or chemical potential gradients requires space coordinates, but see below).

This work focuses on the discussion of such a thermodynamic-kinetic model, with emphasis on the dissolution kinetics of natural repository minerals and crystalline nuclear waste forms such as spent unreprocessed fuel, supercalcine (McCarthy, 1977), THERMALT (Isaacson and Brownell, 1972), and SYNROC (Ringwood, 1978). Such a model would not be directly applicable to the leaching of most glass waste forms at low temperature, because that is generally a transport-dominated process. (See Hench et al., 1979.) Physical systems such as the one this model deals with are often but not always well-approximated by experimental designs using hydrothermal bombs, autoclaves, or other apparatus. Systems in close correspondence with the pure thermodynamic-kinetic model may be closed, or they may be open to certain components (such as O_2 or CO_2 from the air) as long as transport is not rate-limiting.

In the context of a more comprehensive model dealing with a larger system (i.e., the entire near-field zone of a repository) and embodying effects of advection, diffusion, dispersion, and gradients of temperature, pressure, and chemical potentials, the thermodynamic-kinetic model must be applied to compartments, each of which represents part of the volume of the larger system but within which there are no internal space coordinates. This approach has been exemplified already in geohydrologic modeling using finite difference grids (Schwartz and Domenico, 1973; Schwartz and Smith, 1979). A comprehensive model of near-field interactions might also include some compartments possessing internal space coordinates, for example to model the diffusive leaching of waste glass using approaches such as those described by Hench et al. (1979).

2.2 RATE-LIMITING REACTIONS

Ideally, nuclear waste forms would be thermodynamically stable under all credible waste isolation scenarios. There would then exist no driving forces to leach or dissolve the contained radionuclides. Since no waste form (or packaging) is likely to satisfy such a requirement, the degree of <u>kinetic</u> as well as <u>thermodynamic</u> stability is an important factor in assessing its performance in geologic disposal. A particularly important goal of thermodynamic-kinetic modeling is to accurately assess waste package performance in the initial 600-year period when the radiotoxicity of the waste is highest.

Since the principal goal of modeling waste isolation is to assess how waste interacts with packaging, rock, backfill, and chemical buffers, the <u>dissolution</u> kinetics of the solid phases composing these materials should be included in the model. However, only limited provision for <u>precipitation</u> kinetics may be required for practical waste interaction modeling. Most solid phases that precipitate from aqueous solution in response to the dissolution of other solids appear to do so nearly reversibly throughout the overall process (Helgeson, 1968; Helgeson et al., 1969). The dissolution kinetics of the reactant (primary) solids are then solely rate-determining for the whole system, and the system is said to be in a state of partial equilibrium (Helgeson, 1968; Helgeson and Aagaard, 1979). Apart from the scenarios of rapid heating or cooling and of rapid mixing of dissimilar aqueous fluids, only a few solid substances have precipitation kinetics that might be significant for chemical modeling purposes.

More significant to modeling waste interactions may be the slow approach to equilibrium of the redox couples within the aqueous phase (i.e., UO_2^{2+}/U^{4+} may not be instantly at equilibrium with SO_4^{2-}/HS^-). Many redox reactions proceed primarily by the intermediation of biochemical processes rather than inorganic mechanisms (Berner, 1971, Chapter 7; Stumm and Morgan, 1970, Chapter 7). Redox disequilibrium in aqueous fluids may be thought of as the manifestation of unique values of the redox parameters E_h and pe^- for individual redox couples (Thorstenson, 1970, Nordström et al., 1979). Some provision for treating redox kinetics appears necessary to accurately model the behavior of the redox-sensitive radionuclides. The effects of radiolysis in the near-field zone are closely coupled to the role played by aqueous redox

kinetics. This is a consequence of the fact that radiolytic production of highly reducing or oxidizing species (e.g., $Cl_{2(aq)}$) leads to disequilibrium among redox couples.

2.3 METHODOLOGY AND APPLICATION

A fair question to ask is, how does a fundamentally grounded model such as the one proposed here compare with phenomenological studies of waste inter- actions? Each approach has its own goals and merits. We believe these can be managed so as to be complementary. The theoretical model that is the subject of this report will probably never be so fully developed as to make phenomenological studies unnecessary. The philosophy of this, as well as other theoretical approaches in most of science and engineering, is to focus on developing a clear understanding of that minority of phenomena and contraints of a process which determines the majority of its significant results. This is the only practical way to identify and reduce the key uncertainties.

A basic aspect of the modeling process is simplification followed by the development of increasing complexity. This may be manifested not only in the processes and phenomena of interest, but in the systems and substances as well. For example, we may adopt a simple expression describing a process that ignores second-order effects. A good example of this is the perfect gas law. On the other hand, if we wish to predict the behavior of spent unreprocessed fuel, a starting point is to predict the behavior of a compositionally idealized analog or a model spent fuel. The simplest example of this would be pure $UO_{2(c)}$, for which some dissolution simulations are presented later in this report. Such model waste forms can be studied experimentally to measure and confirm their thermodynamic and kinetic properties. Computerized theoretical simulations interact with such experiments by suggesting measurement needs and by confirming the generality and theoretical validity the of measured parameters.

Pure $UO_{2(c)}$ as a model spent fuel is only a first step. Understanding its dissolution gives no direct estimate of the behavior of the other radio- nuclide elements, many of which are more significant than uranium to safety assessment. Spent fuel, apart from cladding, is about 96 to 97 percent UO_2. Therefore, predictions for a pure UO_2 phase are not only a starting point for modeling purposes but may also give qualititative information on the dissolution of the UO_2 phase of actual spent fuel.

- 6 -

A more useful model for spent fuel would include in its composition the other major elements and the most significant minor radionuclide elements present in the actual substance. For example, the chemistry of Pu suggests that it would reside mainly in the UO_2 phase as a diluted (≈ 0.1 percent) PuO_2 end-member. Since this phase in spent fuel would have $\lesssim 3$ percent components in addition to UO_2 and PuO_2, an adequate model spent fuel for predicting the release of Pu might be simply PuO_2-doped UO_2. Similar treatment might suffice for related elements such as Th, Np, Am, and Cm. On the other hand, if most of the Sr, for example, is present in a $(Ba,Sr)ZrO_3$ (or some other) phase, then the release of this element may be only indirectly governed by dissolution of the UO_2 phase. In this case, at least a two-phase model spent fuel is required to assess the hazards of ^{90}Sr.

The gross elemental and isotopic compositions of spent fuels are generally determined by a computer calculation (Bell, 1973) rather than actual analysis. There is unfortunately little information concerning the "mineralogy" and "petrology" of spent fuel. Developing model spent fuels will require detailed information on their actual counterparts, specifically, the phases present, the distribution of elements among the phases, the textural and structural features and relations, and the gradients, if any, that exist within the fuel elements. These considerations also apply to any other general waste form (e.g., glass, supercalcine, THERMALT, SYNROC, tailored ceramics, cements, and cermets).

Chapter 3

DISSOLUTION KINETICS IN AQUEOUS SYSTEMS

3.1 RATE EXPRESSIONS AND MECHANISMS

Irreversible (not at equilibrium) dissolution of a solid compound such as $UO_{2(c)}$ in an aqueous fluid is an example of a process in which thermodynamic driving forces act to cause a system to seek thermodynamic equilibrium. This end may be achieved when either the entire mass of dissolving substance has been destroyed or the system achieves a solubility equilibrium. During the reaction, the fluid composition changes (including its E_h and pH) and secondary precipitates may form and redissolve. If the system is in a state of so-called partial equilibrium, then only the set of irreversible dissolution reactions is rate-limiting and manifests the kinetic rate laws that govern the reacting system as a whole. As discussed earlier, some redox and possibly some precipitation reactions may occasionally also be rate-limiting. However, even in such cases of _limited_ partial equilibrium, the number of kinetic rate laws to be considered need not be very great.

The desirable characteristics of the rate law expressions adopted for waste interactions modeling can be evaluated in light of the requirements of safety assessment. Here modeling serves three functions: (1) to guide experiments (and be in turn guided by them); (2) to show the relations between model parameters and results; and (3) to extrapolate to scales of time, length, and complexity to make predictions for scenarios that can not be directly investigated because of limited time and resources. This last purpose is especially manifested for kinetics modeling by the need to assess the performance of a waste package in the first 1000 years of emplacement and beyond.

Credible predictions for such time scales require that the rate expressions used in the modeling have a strong theoretical foundation. This requires a basic understanding of the governing mechanisms because these expressions must be based on relatively short-term experiments, many of which must be conducted under aggravated conditions (e. g., low pH and/or high temperature). If kinetic stability is adopted as a necessary criterion for an

acceptable waste form, then that substance will by definition dissolve very slowly under repository conditions. In this regard, it would behave similarly to the silicate minerals in natural systems undergoing weathering, diagenesis, and low-grade hydrothermal metamorphism. Important progress has recently been made in understanding the dissolution of mineral silicates. These advances may soon have a strong impact on waste isolation safety assessment in terms of evaluating both waste form performance and waste-rock interactions.

The dissolution kinetics of silicates and many other crystalline substances were until recently thought to be controlled in general by diffusion processes acting in a protective layer of secondary precipitates, gel, or leached lattice (Wollast, 1967; Helgeson, 1971; Paces, 1973; Busenberg and Clemency, 1976). Protection by a layer of secondary material is exemplified by passivation of metals, and the role of leached layers is well established in controlling the alteration of many glasses in aqueous systems at low temperature (Hench et al., 1979, and references therein). However, there is strong evidence that surface reaction mechanisms, not diffusion processes, govern the rate of dissolution of many crystalline substances (Lagache, 1976; Petrovic et al., 1976; Petrovic, 1976; Holdren and Berner, 1979; Berner and Holdren, 1979).

3.2 TRANSITION-STATE RATE EXPRESSION

Aagaard and Helgeson (1977) have proposed the application of transition-state theory (Lin et al., 1975; Boudart, 1976) to describe the rate-limiting step of silicate dissolution. In the Aagaard-Helgeson model, a disrupted configuration of atoms on the surface of the dissolving crystal plays the role of the critical activated complex. The rate expression for the dissolution of feldspar at acid pH in the range 0 to 200 C for the most probable activated complex $\left[(H_3O)AlSi_3O_8(H_3O)^+\right]$ is (Aagaard and Helgeson, 1977)

$$(-dn/dt)_{P,T} = k_{P,T} \, S \, a_{H+} \left[1 - \exp\,(-A/RT)\right]$$

where the following definitions apply:

n = mass of feldspar,

t = time,

P = pressure,

T = temperature, °K,

k = rate constant,

S = surface area over which aqueous solution contacts feldspar,

a_{H+} = activity of hydrogen ion, 10^{-pH},

A = thermodynamic affinity of reaction, and

R = the gas constant.

In the terminology more commonly employed by Helgeson and co-workers (Helgeson, 1968; Helgeson et al., 1970; Aagaard and Helgeson, 1977),

$$d\xi/dt = -dn/dt$$

where ξ, the reaction progress variable, represents the number of moles of substance which have irreversibly dissolved.

The affinity is the thermodynamic driving force of an irreversible reaction. It may be likened to a difference in electrical potentials. It is in fact a difference of chemical potentials. For a reaction of the form

$$wW + xX \rightleftharpoons yY + zZ,$$

the affinity is given by

$$A = w\mu_W + x\mu_X - y\mu_Y - z\mu_Z$$

where μ is the chemical potential function. The affinity is thus similar to the free energy of reaction, but it has the opposite sign. For a reaction to proceed in the forward direction, the affinity must be positive.

A more direct relation to calculate the affinity is

$$A = - 2.303 \ RT \ \log Q/K = 2.303 \ RT \ (\log K - \log Q)$$

where Q is the activity product of the reaction and K is the corresponding equilibrium constant. In terms of the reaction written above,

$$\log Q = y \log a_Y + z \log a_Z - w \log a_W - x \log a_X$$

$$\log K = - \ (Y\Delta G^O_{fY} + z\Delta G^O_{fZ} - w\Delta G^O_{fW} - x\Delta G^O_{fX})/2.303RT$$

where "a" is thermodynamic activity and ΔG^O_f the standard-state Gibbs energy of formation from the elements.

Computer codes that generate thermodynamic models of aqueous systems compare Q and K to estimate the degree of supersaturation or undersaturation of the fluid with respect to a mineral. One saturation index commonly used is log Q/K, which is a dimensionless form of the affinity of the <u>precipitation</u> reaction (reversing the direction in which a reaction is written reverses the sign of its thermodynamic properties). Thus, for a <u>dissolution</u> reaction, we have the following saturation index conventions:

$\log Q/K > 0$	supersaturation
$\log Q/K = 0$	saturation
$\log Q/K < 0$	undersaturation

which are opposite in sign to those of the affinity of dissolution:

$A < 0$	supersaturation
$A = 0$	saturation
$A > 0$	undersaturation

3.3 PRACTICAL KINETIC MODELING

The Aagaard-Helgeson model of dissolution kinetics is simple in form and therefore well-adapted to modeling purposes (Compare some of the expressions

for modeling sorption given by James and MacNaughton, 1977; Davis et al., 1978; Westall and Hohl, 1980; and references therein). Secondly, it is consistent with thermodynamics (Boudart, 1976) and the limiting approach to thermodynamic equilibrium ($-dn/dt \rightarrow 0$ as $A \rightarrow 0$). We may compare its general form with that of the following rate law for the dissolution of uraninite under oxidizing conditions proposed by Grandstaff (1976), given here for the pure substance and in our notation:

$$- dn/dt = k\ S\ a_{H+}\ a_{\Sigma CO_2}\ a_{O_2(aq)}$$

The form of this expression is a manifestation of a numerical regression model not based on any specific mechanistic understanding of the dissolution process. It is, in essence, a device for interpolating between measurements. Note that the transition-state model is no more difficult to employ. Grandstaff's equation, however, would predict a positive rate of dissolution in a supersaturated solution if used outside its proper context. The Aagaard-Helgeson expression, because of its consistency and strong base in theory, appears suited for extrapolation, that is, for making predictions of interactions in aqueous systems over 1000-year time scales (Helgeson and Aagaard, 1979).

Unfortunately the notion of diffusion-controlled dissolution kinetics has persisted until so recently that few if any experimental measurements have been made with transition-state or any other surface-mechanism theory in mind. In general, the affinity function must be calculated from a thermodynamic model that requires an essentially complete description of the aqueous solution. Most published studies of dissolution rates (of minerals or of waste forms) do not provide this. New experimental studies will be required to provide both the necessary measurements and to establish the exact form of the rate law for each substance. For example, the specific form for feldspar dissolution proposed by Aagaard and Helgeson (1977) has the activity of the hydrogen ion (a_{H+}) preceding the affinity factor. More generally, this pre-affinity factor is an activity product defined by the nature of the activated complex. The activities of the hydrogen ion, the solvent (H_2O),

and the electron (recall that $pe^- = -\log a_e$), and perhaps other aqueous species, may appear here raised to appropriate powers.

In the absence of a realistic kinetic rate law, one may construct a partial equilibrium model of irreversible dissolution using arbitrary rate expressions (Helgeson, 1968; Helgeson et al., 1970; Wolery, 1979a). Here one uses the reaction progess variable (number of moles of substance irreversibly dissolved) in place of time as a measure of how far a reaction has proceeded. If there is only one such irreversibly dissolving substance, one may apply this technique and then integrate the correct kinetic rate expression a posteriori to determine ξ in terms of time. Helgeson and Aagaard (1979) applied this technique to simulations of feldspar dissolutions and termed it a "retroactive clock." In particular, they showed that ξ and t are not normally linear with respect to each other.

Arbitrary kinetics is not a completely satisfactory substitute for real kinetics, however. Consider a system containing two irreversibly dissolving substances. Letting ξ_1 and ξ_2 describe their respective extents of reaction progress, one must then specify their relative rate of dissolution:

$$\frac{d\xi_1}{d\xi_2} = \frac{d\xi_1/dt}{d\xi_2/dt}$$

In arbitrary kinetics, this ratio is usually specified as a constant whose value is arbitrarily chosen. Even if one knew the correct value at the start of the reaction, it would undoubtedly change in a real system as the reaction progressed. This aspect of irreversible dissolution therefore requires a priori specification of realistic kinetic rate laws to properly model such systems.

Chapter 4

SOLID SOLUTION IN WASTE INTERACTIONS

The compositions of many solid phases important to waste isolation studies (including natural minerals, some proposed backfill/buffer materials, and waste forms, such as SYNROC) are not constrained by their intrinsic nature to narrow ranges. Rather, they exhibit a considerable range of allowed substitution of one ion for another. This is perhaps best exemplified by those minerals with the highest "sorption" capacities (zeolites, smectites, and vermiculites). These phases exhibit a wide range of mixing of cations (e.g., Na^+, K^+, Cs^+, Mg^{2+}, Ca^{2+}, Sr^{2+}, usually hydrated) in channel sites (zeolites) or interlayer sites (smectites and vermiculites). Solid solution also manifests by substitutions among ions on sites for which rapid ion exchange with aqueous solution does not occur. In smectites and vermiculites, for example, Al^{3+}, Fe^{3+}, and Si^{4+} substitute for one another on tetrahedral sites in the sheet silicate lattice, while Al^{3+}, Fe^{2+}, and Mg^{2+} do likewise on octahedral sites.

The thermodynamics of solid solutions may be described by specifying the properties of a set of end-member components and a set of relations that describe how the properties of the end-members change in the process of mixing to form solid solution. The choice of end-members is usually straightforward, but two different approaches may be applied to describing the mixing relations (for example, see Powell, 1978, Chapter 4).

The first procedure is based on the concept of molecular mixing, which is appropriate for describing gas mixtures. This approach to describing solid solutions has been extensively discussed elsewhere (Garrels and Christ, 1965, pp. 42-49; Berner, 1971, p. 21; Helgeson et al., 1970; Stumm and Morgan, 1970, pp. 205-212; and sources cited therein). The chemical potential of the i-th component is written

$$\mu_i = \mu_i^o + RT \ln x_i \lambda_i$$

where μ_i^o is the chemical potential of the pure end-member at the temperature

and pressure of interest, R is the gas constant, T the absolute temperature, x_i the mole fraction in solid solution, and λ_i the activity coefficient. In the _ideal_ version of this model, $\lambda_i = 1$ always. The basic problem with this approach is that the end-members generally do not mix in the molecular sense. Hence the activity coefficients differ significantly from unity and are difficult to predict.

A more realistic approach recognizes that in crystal structures ions mix over sites (Powell, 1978, Chapter 4; Helgeson et al., 1978; Kerrick and Darken, 1975; Ulbrich and Waldbaum, 1976; and sources cited therein). In this model, the chemical potential of the i-th end-member is written

$$\mu_i = \mu_i^o + \left\{ RT \sum_{jk} \sum \ln x_{j,k} \, \lambda_{j,k} \right\} / N_i$$

where $x_{j,k}$ is the mole fraction of the k-th ion on the j-th site, $\lambda_{j,k}$ is the corresponding activity coefficient, and N_i is a normalization constant whose value may be obtained by solving the equation for the case of the pure end-member. The k-th "ion" may be a vacancy or a real ion. The ideal solution in this context has each $\lambda_{j,k} = 1$ always. In many cases, the ideal site-mixing model gives results in good accord with experimental data (Helgeson et al., 1978). Evaluation of the right-hand-side of the site-mixing equation is sometimes straightforward, but if pairs of ions can exchange from different sites, one must first evaluate intracrystalline equilibria that parallel those for the dissociation of complexes in aqueous solution.

Site-mixing models have been applied more extensively in metallurgy (Oates, 1969; Pelton et al., 1979) and high-temperature petrology (Powell, 1978, Chapter 4; Blander, 1972; Ganguly, 1977) than in the branch of geochemistry dealing with aqueous systems. The approach has recently been applied, however, to such low-temperature minerals as clays (Stoessell, 1979; Aagaard et al., ms. in prep. cited by Helgeson et al., 1978). Unfortunately, the major computer programs used in chemical modeling of aqueous systems (REDEQL, MINEQL, SOLMNEQ, WATEQ2, PATHI, EQ3/EQ6; see Nordstrom et al., 1979 for detailed references) either deal only with pure mineral compositions or permit only molecular mixing models of solid solution.

The incorporation of site-mixing models into chemical modeling codes appears to be both desirable and necessary for waste interactions studies. Many components of interest in such studies will be present as minor or trace constituents even in the near-field environment. It will be difficult to accurately predict the behavior of many of them without a realistic treatment of solid solution phenomena. Furthermore, the dissolution kinetics of crystalline waste forms such as spent unreprocessed fuel or SYNROC will be affected by their solid solution thermodynamics through the contribution of the free energy of mixing to the affinity function discussed in Chapter 3.

Chapter 5

EQ3/EQ6 CODE PACKAGE*

5.1 DESCRIPTION

The EQ3/EQ6 code package is a general geochemical thermodynamic modeling
package that was originally written by Wolery (1978) at Northwestern University
and subsequently further developed and described by Wolery (1979a) at Lawrence
Livermore National Laboratory. It simulates irreversible reaction in aqueous
systems according to the theoretical constraints developed by Helgeson (1968)
and Helgeson et al. (1970). It has previously applied to model rock-water
interactions in mid-oceanic ridge hydrothermal systems (Wolery, 1978), geo-
thermal resources (Taylor et al., 1978; Wolery, 1979b), and formation of copper
ore deposits (Brimhall, 1979). Here we describe progress in using this code
package to develop a capability to model interactions of nuclear waste in
geologic disposal scenarios.

A detailed description of the code package prior to its adaptation to
nuclear waste isolation modeling is given in UCRL-52658 (Wolery, 1979a).
Errata for that report are given in Appendix A of this report. Here we briefly
describe the elements of the code package and point out work done to improve
them since the publication of UCRL-52658. The package consists of two main
codes (EQ3 and EQ6), supporting data files, and data file management routines.

EQ3 computes a speciation model for the solutes in an aqueous solution,
that is, it estimates the extent of ion-pairing and complex formation. Its
results are required to initialize EQ6 calculations. It is otherwise similar
in function to such codes as WATEQ, WATEQ2, SOLMNEQ, REDEQL, MINEQL, and
GEOCHEM (Nordstrom et al., 1979, and references therein). Apart from modeling
the speciation, the major function of such codes is often to calculate the

---

*The EQ3/EQ6 code package is available for public distribution from the
 National Energy Software Center, Argonne National Laboratory, 9700 South Cass
 Avenue, Argonne, Illinois, U.S.A. 60439. Released versions are updated
 periodically.

degree of disequilibrium between the solution and various solid phases (i.e., estimate the function log Q/K for these phases).

EQ6 is a reaction progress code. It computes numerical simulations of irreversible dissolution using arbitrary kinetics (Chapter 3). It was written to be a second-generation reaction-progress code to replace the original PATHI program (Helgeson, 1968; Helgeson et al., 1970). Wolery (1979a) discusses the improvements that were effected. EQ6 simulates three physical model systems that will be discussed later in this report.

5.2 RECENT DEVELOPMENT

The EQ3 and EQ6 codes are both written in the style of generalized coding. Adding a new element, aqueous species, or solid does not require modification of the source codes, except perhaps to increase the size of the appropriate arrays. Since the publication of UCRL-52658, both codes were modified to eliminate the reading into memory of supporting data not needed in a given run. This was necessary to minimize the size of arrays so as to reduce inefficiency and avoid exceeding physical and administrative memory limitations as the size of the supporting data base increased in response to the needs of waste interactions modeling.

The EQ3 code was also significantly modified by adding a basis-switching capability required to overcome nonconvergence problems that arose when an aqueous complex, such as $UO_2(CO_3)_2^{2-}$, is so stable that the concentration of a constituent simple ion, such as UO_2^{2+}, is negligible by comparison. This feature is also sometimes needed to exchange the roles of simple constituent ions of the same element in different valence states, such as U^{4+} and UO_2^{2+}, when one is negligible compared to the other. Basis-switching consists essentially of rewriting elementary chemical reactions so that reactions normally written in terms of certain simple ions, such as UO_2^{2+}, are instead written in terms of alternate species, such as U^{4+} or $UO_2(CO_3)_2^{2-}$. EQ3 is written to allow the user to specify basis switching on the input, but also has an automatic basis-switching feature. The numerical techniques of EQ6 appear to be relatively indifferent to the manner in which reactions are written. At the present time, it merely follows the basis selection of EQ3.

The data base is organized to support calculations over the temperature range 0 to 300 C, which is sufficient for most waste isolation scenarios. When UCRL-52658 was published, the data base lacked many of the chemical elements prominent in nuclear waste (especially, Sr, Cs, Tc, U, Pu, and other actinides). A major expansion of the data base was therefore initiated. As part of the expansion completed to date, 38 new aqueous species and 25 new minerals were added as a consequence of adding one new element, uranium. Addition has been started but not completed for the elements Sr, Cs, Zr, Ba, V, P, N, and F. Sr and Cs isotopes are major fission products in nuclear waste; Zr is cladding on spent unreprocessed fuel; and Ba, V, P, N, and F are elements that may participate in significant interactions with radionuclides in geologic disposal scenarios. Other chemical elements are planned for inclusion in the future.

Most 25 C data for U species and compounds were taken from the critical compilation of Langmuir (1978). Heat capacity coefficients for solid compounds, along with 25 C Gibbs energies, enthalpies, and entropies for a few solids not given by Langmuir, were taken from Barin and Knacke (1973), Barin et al. (1977), and Kubaschewski and Alcock (1979). Checks were made to ensure consistency among these sources and with Helgeson and Kirkham (1974a, 1974b, 1976) and Helgeson et al. (1978). The latter works are the sources of most of the data in the EQ3/EQ6 data base as of the publication of UCRL-52658.

Data base expansion was facilitated by using the codes of Barner and Scheuerman (1978) to extrapolate thermodynamic data from 25 C to high temperatures. These codes use the algorithms of Criss and Cobble (1964a, 1964b) and of Helgeson (1967) to approximate the heat capacity functions of aqueous species. A new code, EQUTLK, was created to format the ouput of the former codes (Gibbs energies on a temperature grid) into log K values for reactions. The utility codes in the previous EQ3/EQ6 package, EQF and EQS (Wolery, 1979a) were combined into a single code EQUTIL. This code fits interpolating polynomials to the data on the temperature grid and writes the coefficients on files that directly support EQ3 and EQ6.

5.3 REACTION-PROGRESS MODEL SYSTEMS

Reaction-progress calculations made by the EQ6 code correspond to one of three simple physical models. The first is the titration process depicted in Fig. 1. The flask contains a system of aqueous fluid and solid phases. This system is in a state of complete heterogeneous thermodynamic equilibrium, i.e., the solution is exactly saturated with each solid present. Outside the flask there is a different solid (the "reactant"), which is not in equilibrium with the system in the flask.

Reaction-progress simulations in geochemistry have usually been performed for scenarios which involve only rock and aqueous fluid. Figures 1 and 2 depict a system open to the atmosphere. Reactions among minerals and aqueous solutions may be greatly sensitive to the presence of a gas phase. In our discussion here, we focus on the simple case in which a gas phase is not present (in contrast to the implications of Figs. 1 and 2), or alternatively assume that the significant reactions among aqueous solutions and minerals are independent of mass transfer between aqueous and gaseous fluid phases (which in fact is not often likely). Mass transfer involving a gas phase can be treated in the theoretical formalism of this modeling methodology, but provision for doing so has not yet been made in the current EQ3/EQ6 software.

The reactant is added to the flask in small increments. Upon each addition, the increment of reactant dissolves and perturbs the existing state of equilibrium. The system then reequilibrates, seeking a new equilibrium state corresponding to its new elemental composition. This yields a new composition of the aqueous fluid (including new pH and new E_h). Some of the product solids may have increased or decreased in mass. New such solids may have appeared and old ones may have disappeared. This process may be repeated until there is no remaining reactant material or the fluid reaches a solubility equilibrium with it.

A closely related model is irreversible reaction in a closed system, illustrated in Fig. 2. Instead of adding small increments of reactant to the flask, we put in a single large mass. It then dissolves according to its own governing rate law. One may think of this process as occurring by the sequential dissolution of discrete layers, whose masses are comparable to those of the incremental masses in the titration model. If this irreversible dissolution is the only rate-limiting reaction in the system, then the system is in a state of partial equilibrium.
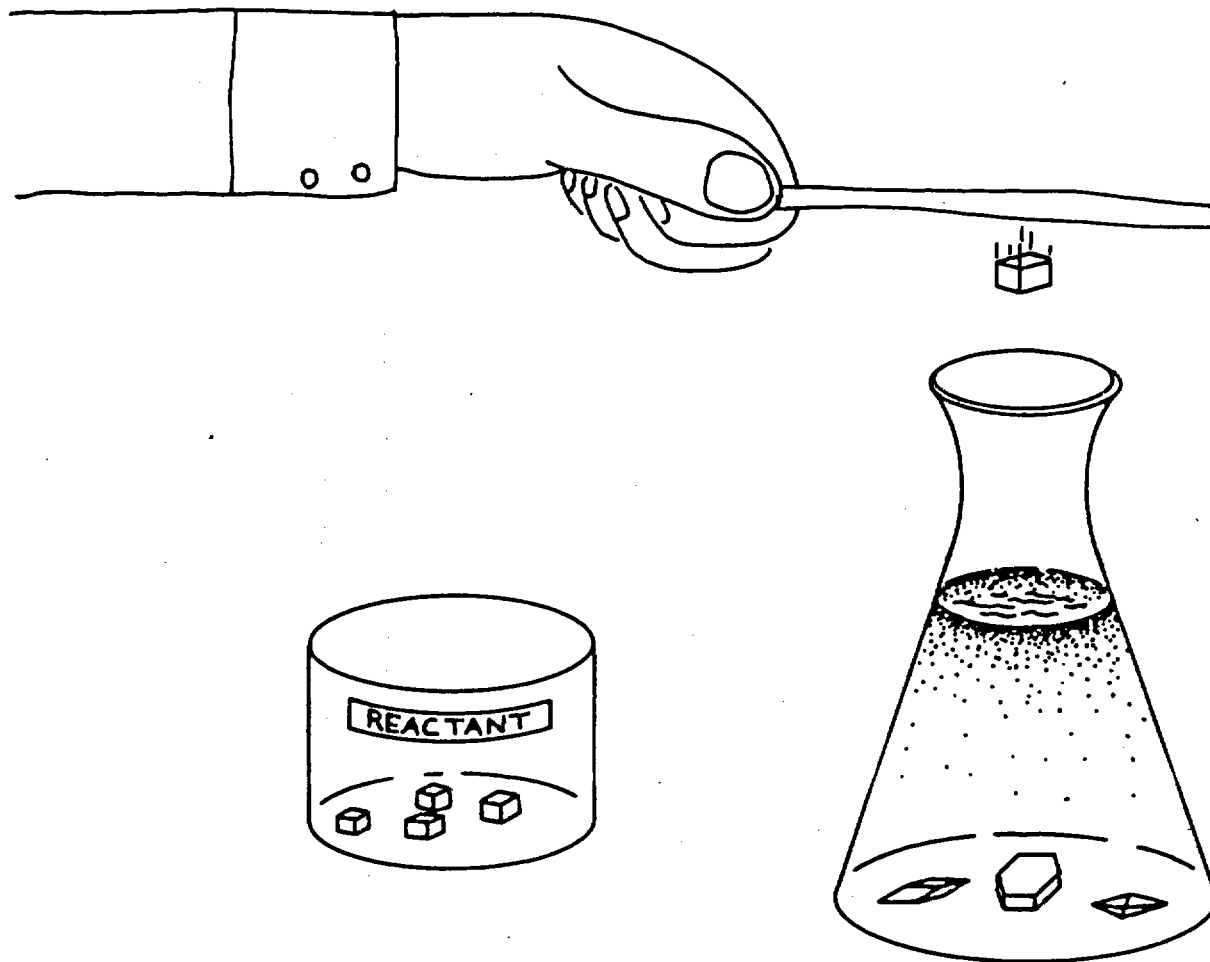
- 22 -

FIG. 1. Titration of an aqueous system (flask) by a reactant substance (small cubes). Secondary or product solids (bottom of flask) form by equilibrium precipitation. Mass transfer to and from the overlying gas phase is assumed to be negligible in the simplest case discussed in the text.
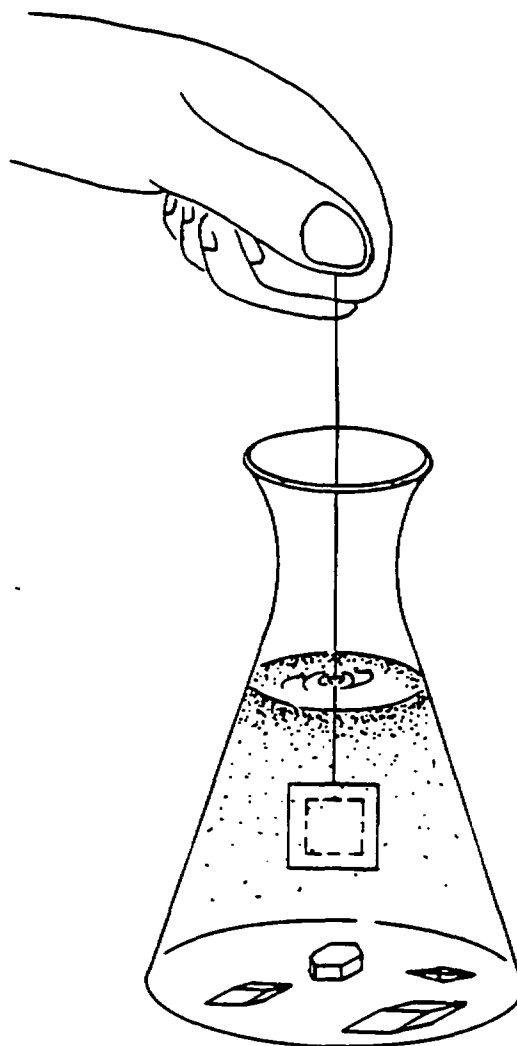
FIG. 2. Irreversible reaction of a reactant substance (large cube) in a closed aqueous system (flask). Mass transfer to and from the overlying air is taken to be negligible in the discussion of the model in its simplest case.

There is a high degree of similarity between the titration and closed system models. In fact, they may often give exactly the same results. A subtle difference, however, may arise (but not always) when there is more than one reactant present. In general, multiple reactants will not saturate the aqueous fluid simultaneously. If one reactant saturates but another does not, the simulation continues. In the titration model, the saturated reactant continues to be incremented into the system as before, but in the closed system model any remaining mass of saturated reactant changes to product mineral status. Thus far, the results from the two models could still be identical. The difference arises if the fluid should later become unsaturated with a once-saturated reactant. In the titration model, irreversible dissolution of this substance might recur later; in the closed system model, it could only be destroyed reversibly (while maintaining a solubility equilibrium).

A third physically simple model (Fig. 3) is a flow-through system. It is a special kind of open system that follows the evolution of a packet of aqueous solution as it passes through a medium. This medium could be a fracture, as depicted in Fig. 3, a porous medium, or a pipe (e.g., a geothermal reinjection well; Wolery, 1979b). Reactant solids that contact the fluid dissolve irreversibly, as in the closed system, but the product minerals adhere to the medium and are thus physically separated from the fluid packet from which they precipitated. The flow-through model may also include the effect of the fluid packet experiencing a temperature gradient. This may be useful in evaluating waste interactions, because fluid approaching a young repository will heat up and then cool as it moves away.

One might be tempted to associate the closed system with most laboratory experiments and the simple flow-through system with the situation in the geologic environment. We have earlier addressed the role of the closed system within the framework of compartmentalization and superimposition of transport processes. However, the closed system is in addition a better approximation to geologic reality by itself than the flow-through system if fluid recirculates along the same pathlines within the saturated zone and thus reencounters previously precipitated product phases. The flow-through model is appropriate only for the case of a fluid not traversing its former pathlines (Villas and Norton, 1977).
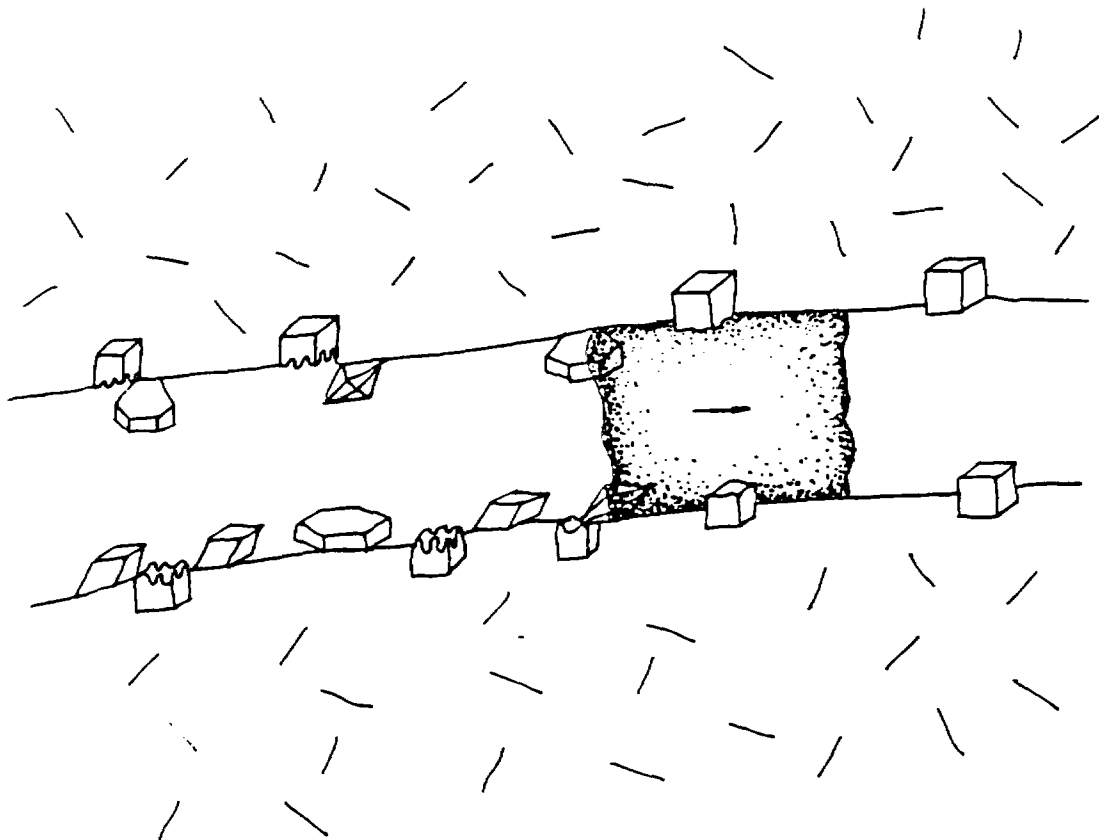
FIG. 3. Irreversible reaction of a reactant substance (cubes) lining a fracture with a flowing packet of aqueous solution. Product minerals adhere to the fracture walls while the fluid packet moves on.

Chapters 5 and 6 of this report demonstrate the utility of the modeling code package (EQ3/EQ6) in gaining an understanding of waste interactions. In particular, we point out the limitations of this approach and how they can be ameliorated by appropriate activities of further code development and experimental measurements. We look first at waste-rock interactions, and then at waste-container-rock interactions.

Chapter 6

MODELS OF UO_2 DISSOLUTION IN GRANITIC GROUNDWATER

6.1 INTRODUCTION

The expanded data base has been used to make some simulations of the
dissolution of $UO_{2(c)}$, the simplest model spent fuel, in groundwaters that
might be found in a hard-rock repository. Because of the general lack of
comprehensive analyses of groundwaters in the literature, it was necessary to
construct hypothetical compositions based on reported values for a number of
different actual samples. (See White et al., 1963, for one of the few
compilations of groundwater compositions.) The compositions used here are
intended to represent fluids that might be found in a granitic terrain.

Three versions of a granitic groundwater, differing only in redox state,
are presented in Table 1. The major element chemistry is constructed mainly
after an analysis reported by Fritz et al. (1978, Table 3, Well 3-74). At 25
C, these groundwaters are just saturated with quartz and kaolinite, which are
major alteration products of granite weathering. We assume that redox
equilibrium holds among all couples so that the fluid redox state is described
by a single value of E_h and that the reacting systems are, in a state of
partial equilibrium as discussed in an earlier section. The first groundwater
is saturated with atmospheric oxygen (the most oxidizing case). The second is
only moderately oxidizing, and the third is fairly reduced. The latter may or
may not best represent deep-seated groundwaters, whereas the first two at
least represent fluids originally near the surface that might invade a
repository.

Simulations of the dissolution of UO_2 in each groundwater in closed
systems were performed for temperatures of 25, 100, 200, and 300 C. We
therefore emphasize the important roles of redox state and temperature in
governing UO_2 dissolution. Other important parameters, such as the
concentrations of certain complexing ligands, especially CO_3^{2-} and SO_4^{2-},
will also become apparent. Fluoride, phosphate, and organic anions may also
be of some significance to uranium geochemistry, but they were omitted from
these simulations because of their incomplete representation in the thermo-
chemical data. base. Work to overcome these deficiencies is in progress.

TABLE 1. Hypothetical composition of oxidizing, moderately oxidizing, and reduced granitic groundwater at 25 C.

| Parameter	Value	
E_h	$+ 0.781$	oxidizing
	$+ 0.745$	moderately oxidizing
	$+ 0.086$	reduced
pH	7.4	
Na^+	120	μ molal
K^+	28	
Ca^{2+}	200	
Mg^{2+}	124	
Si^{4+}	96.8	
CO_3^{2-}	390	
Cl^-	186.9	
SO_4^{2-}	130	
Al	0.0084	(0.23 ppb)
U	0.01	(2.34 ppb)
Cu	0.01	(0.64 ppb)
Pb	0.01	(2.07 ppb)

When an aqueous solution is heated or cooled, its E_h and pH may change, and it may become supersaturated with certain solids and precipitate them. The initial (prior to UO_2 dissolution) high-temperature solutions here were established by simulating heating from 25 C. Negligible amounts of antigorite, $Mg_{48} Si_{34} O_{85} (OH)_{62}$, and sometimes kaolinite, $Al_2Si_2O_5(OH)_4$, appeared in this step. Anhydrite ($CaSO_4$) appeared at 300 C in significant quantity relative to the dissolved Ca^{2+} and SO_4^{2-} at 25 C. All such initial precipitates were removed from the system before starting UO_2 dissolution. This was an arbitray choice; the modeling code does not require that this be done. As we will see later, leaving the initial anhydrite present in the 300 C simulations would have given different results.

The most important factors in determining the level of dissolved uranium that may be attained by reaction of spent fuel or uraninite with groundwaters are (1) the presence of strong oxidants, chiefly $O_{2(aq)}$, (2) the concentrations of strongly complexing ligands (especially, carbonate, sulfate, and other anions), and (3) the low solubilities of uranium oxides (UO_2; U_4O_9; $\alpha-U_3O_8$) and uranyl hydroxides or hydrated oxides [schoepite, $UO_2(OH)_2 \cdot H_2O$, and $\beta-UO_2(OH)_2$]. The salinity of the groundwater has much less influence on the equilibrium level of dissolved uranium than would be the case for many other metals. This level is quite sensitive to the concentrations of species such as $O_{2(aq)}$, H+, and ligands (e.g., CO_3^{2-} and OH^-). However, none is a major brine salt component, so the range of effects for dilute groundwaters should basically overlap that for concentrated brines.

Note that pH and the oxidation-reduction potential E_h may figure more or less directly in all three factors above. Instead of E_h, the redox state may be quantified by the conventional electron activity function pe^- ($-\log a_{e-}$), the oxygen fugacity, or the concentration of dissolved oxygen. E_h and pe^- are related by

$$E_h = \frac{2.303RT}{F} pe^-$$

where F is the Faraday constant, R the gas constant, and T the absolute temperature. For the half-reaction

$$1/2\ H_2O_{(\ell)} \rightleftharpoons 1/4\ O_{2(aq)} + H^+ + e^-$$
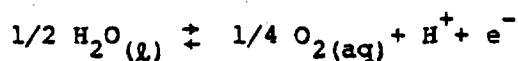
the potential is

$$E = \frac{2.303RT}{F}(1/4 \log a_{O_{2(aq)}} - pH - 1/2 \log a_{H_2O} - \log K)$$

where "a" denotes the thermodynamic activity of a species (pH = $-\log a_{H+}$) and K is the equilibrium constant for the half-reaction. E may be taken as the E_h of the above half-reaction by adopting the usual thermodynamic conventions (Note: these conventions are generally stated only for 25 C; Wolery, 1980, ms. in prep., clarifies the conventions defining E_h and pe^- that are used in this study, particularly with regard to their extension from 25 C and 1 bar to high temperature and pressure). In dilute groundwaters, the activity of a

neutral species such as $O_{2(aq)}$ is nearly equal to its molal concentration m and $\log a_{H_2O} \approx 0$. Under these conditions,

$$E_h \approx \frac{2.303RT}{F} (1/4 \log m_{O_{2(aq)}} - pH - \log K)$$

Analogous equations relate E_h to the oxygen fugacity.

In the following simulations, reaction progress (or in a sense, time) is measured by the amount of UO_2 that has irreversibly dissolved in an aqueous phase initially containing one kilogram of solvent $(H_2O_{(\ell)})$. The amount of solvent produced or destroyed in these simulations is negligible. Enough UO_2 is presumed present in closed system to saturate the fluid. Partial equilibrium is assumed to hold throughout the process.

6.2 OXIDIZING GROUNDWATER

The major consequences of irreversible dissolution of UO_2 in the oxygenated granitic groundwater at 25 C are shown in Fig. 4. The E_h, total dissolved uranium, and masses of alteration solids are depicted as functions of how much UO_2 has dissolved. At the present time, we must use this as a measure of time itself. There is experimental evidence which suggests that the rate of UO_2 dissolution would be about 2×10^{-5} g UO_2/cm^2-day in the oxidizing region (Grandstaff, 1976). However, we know of no reliable rate measurements that apply to reducing conditions.

The top of Fig. 4 shows that E_h is strongly positive (+0.78 volt) until the dissolved oxygen has been effectively exhausted. Once this component becomes insignificant, there is little redox buffer capacity, and E_h drops precipitously to a much lower value. It is buffered then by the presence of two secondary solids, schoepite $\left[UO_2(OH)_2 \cdot H_2O\right]$ and $\alpha-U_3O_8$ (Fig. 4, bottom). Later, all the schoepite is dissolved and E_h drops to a still lower level where it is buffered by $\alpha-U_3O_8$ and a new product solid, U_4O_9. Near the end of the reaction, all the $\alpha-U_3O_8$ is dissolved; the E_h again drops precipitously, this time reaching equilibrium with UO_2. At this point, the overall reaction ceases, and we are left with a reduced groundwater, any remaining undissolved UO_2, and some secondary U_4O_9.
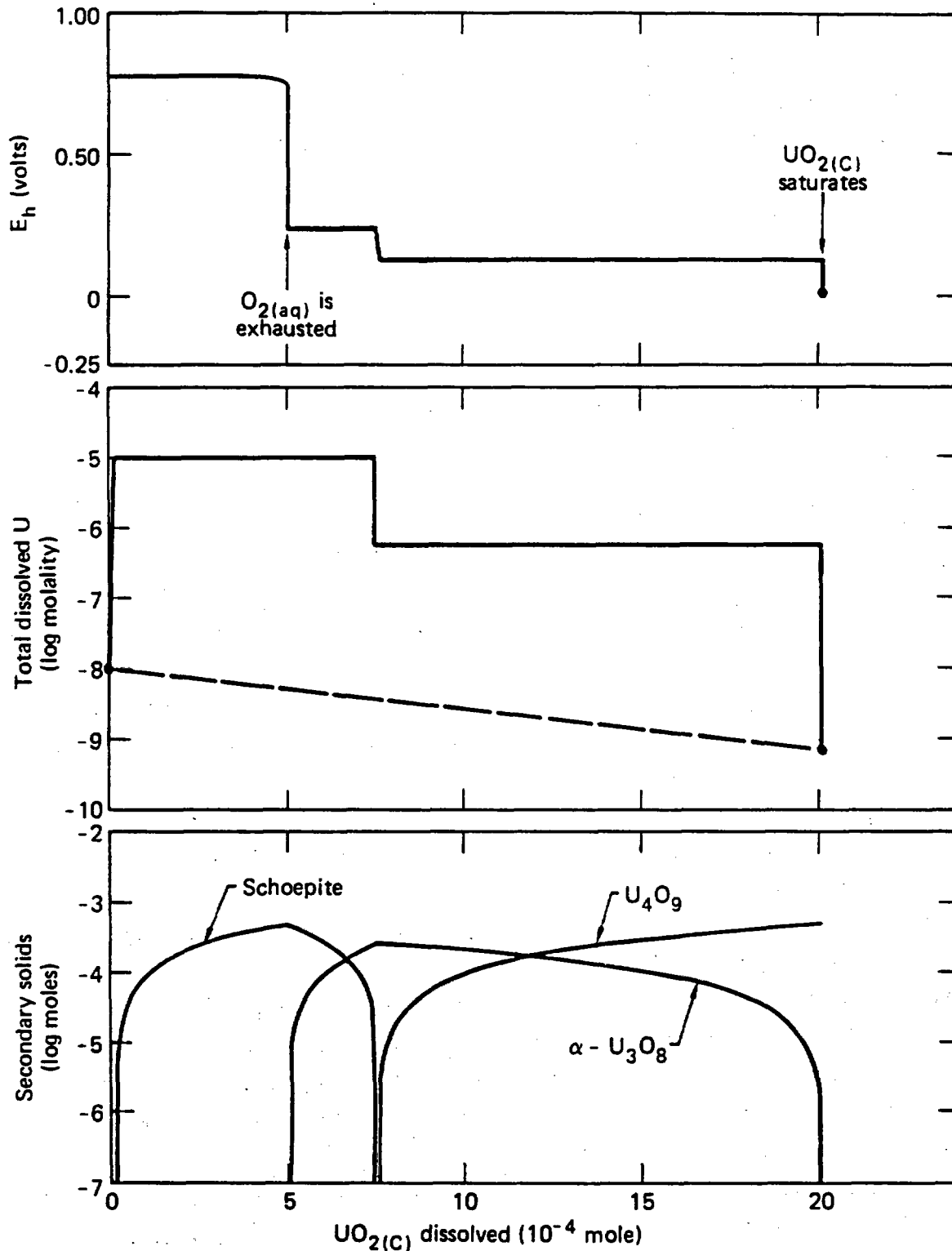
FIG. 4. Redox potential (E_h), dissolved uranium, and secondary solids produced by dissolution of $UO_{2(c)}$ in oxidizing granitic groundwater at 25 C.

The pH in this simulation, and in the other simulations at 25, 100, and 200 C, remains constant to three significant figures at the initial value. The initial value, however, does depend on the temperature. Because of the essential constancy of pH in these dissolution simulations,

$$\log m_{O_2(aq)}$$

is nearly proportional to E_h. With changes of scale in the ordinate of Fig. 4, top, this would also be a plot of

$$\log m_{O_2(aq)}$$

or pe^- against reaction progress.

Total dissolved uranium (Fig. 4, middle) rises quickly from 10^{-8} molal to 10^{-5} molal in the initial part of the reaction, where UO_2 dissolves congruently. A solubility limit is then imposed by precipitation of schoepite. This solid reversibly dissolves when $\alpha-U_3O_8$ also appears (Fig. 4, bottom) and competes with it for uranium. When all the schoepite is dissolved, the level of dissolved uranium can no longer be maintained. It drops along with the E_h until U_4O_9 also appears, and is then buffered at a lower level by $\alpha-U_3O_8$ and U_4O_9. When the $\alpha-U_3O_8$ is completely dissolved, dissolved uranium again follows E_h in dropping precipitously to the point of UO_2 saturation. When this is reached, dissolved uranium is less than 10^{-9} molal, and the groundwater has less than one-tenth of its initial uranium content (emphasized by the dashed line, Fig. 4, middle).

Only two of the minerals in the sequence schoepite- $\alpha-U_3O_8-U_4O_9-UO_2$ may be in simultaneous equilibrium with the aqueous fluid. This is made clear by a plot of their mutual phase relations in E_h-pH space (Fig. 5). At 100 C and higher temperatures, the same restrictions apply although schoepite is replaced in the sequence by $\beta-UO_2(OH)_2$.

The significant consequences of UO_2 dissolution in the same groundwater but at 100 C are shown in Fig. 6. The E_h (top) follows the same pattern, although the values (including the initial value) are slightly lower as a result of the change in temperature. The pattern of dissolved uranium is also very similar to that at 25 C, although the two plateau values are smaller. As we will point
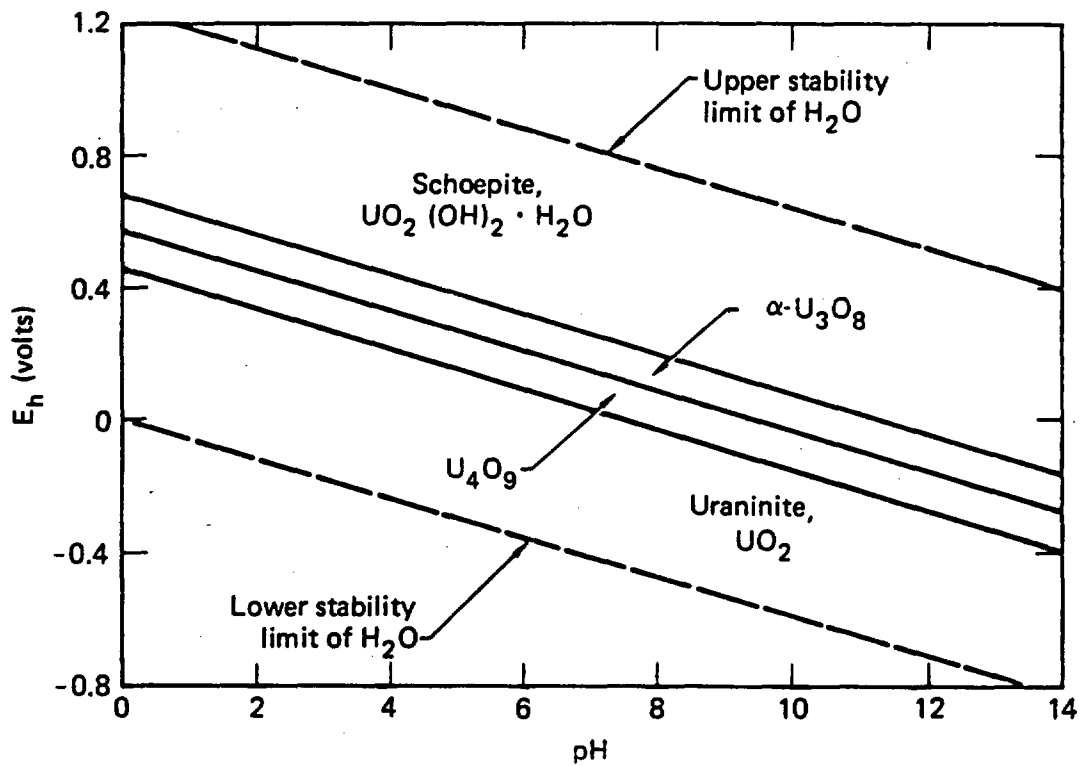
FIG. 5. Pourbaix (E_h-pH) diagram showing phase relations among schoepite, α-U_3O_8, U_4O_9, and UO_2 at 25 C and 1.013 bar.
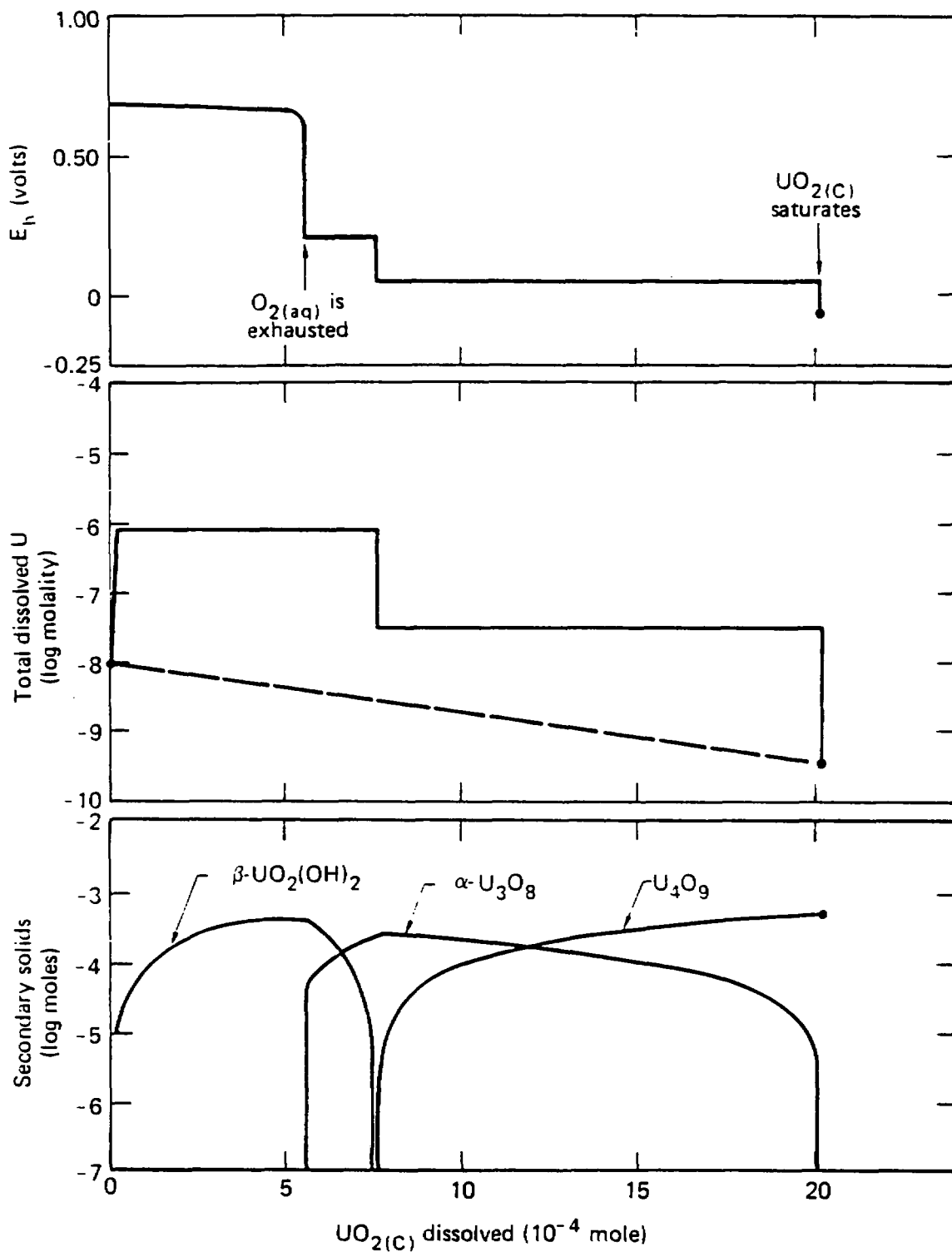
FIG. 6. Redox potential (E_h), dissolved uranium, and secondary solids produced by dissolution of $UO_{2(c)}$ in oxidizing granitic groundwater at 100 C.

out later, this is a consequence of the decreasing relative stability of the uranyl carbonate complexes with increasing temperature. The only remaining significant difference from the 25 C simulation is that β-$UO_2(OH)_2$ has taken over the role of schoepite.

Dissolved uranium as a function of reaction progress for simulations of UO_2 dissolution in oxidizing groundwater at 25, 100, 200, and 300 C are shown in Fig. 7. Note that we now use a logarithmic abscissa. The same sequence of secondary solids appears at 200 and 300 C as at 100 C. At 200 C, dissolved uranium lies on or below the 100 C curve, continuing the earlier trend. The 300 C curve behaves in an unexpected fashion. Instead of falling on and below the 200 C curve, it lies on and above that for 25 C.

The speciation of dissolved uranium at 25 C is shown as a function of reaction progress in Fig. 8. The three uranyl carbonate complexes account for more than 90 percent of all dissolved uranium from start to finish. Uranyl sulfate complexes are of very minor significance. The decreases in the maximum levels of dissolved uranium with increasing temperature seen in the 25, 100, and 200 C runs are due to the decreasing relative stability of the uranyl carbonate complexes which make up most of the dissolved uranium in these simulations. The stabilities of these complexes have been determined experimentally to 200 C (by Sergeyeva et al., 1972; data revised by Langmuir, 1978) rather than extrapolated from 25 C, as is the case for most aqueous complexes.

The speciation of dissolved uranium as a function of reaction progress at 300 C, (Fig. 9) is quite different from that of the lower temperatures. Dissolved uranium consists almost entirely of the two uranyl sulfate complexes. The method of extrapolating thermochemical data for uncharged aqueous species such as $UO_2SO_4^o$ and $U(OH)_4^o$ (Helgeson, 1967) is recommended for use up to only 200 C. EQ3/EQ6 takes such data for 100, 150, and 200 C and performs finite-difference extrapolations for temperatures above 200 C (it interpolates for lower temperatures). However, experimental measurements from 25 to 200 C (Lietzke and Stoughton, 1960) support the stability data for the uranyl sulfate complexes.*

---

*As this report was going to press, the author received a preprint of a paper by R.J Lemire and P.R. Tremaine (1980, J. Chem. Eng. Data, in press) which cites experiments of N.M. Nikolaeva (1971, Izv. Sib. Otd. Akad. Nauk SSSR, Ser. Khim. Nauk, (3), 61). Nikolaeva's results in the range 100 to 150 C show markedly less complexing between UO_2^{2+} and SO_4^{2-} than that reported by Lietzke and Stoughton (1960). At the present time we know of no clear explanation of this discrepancy.
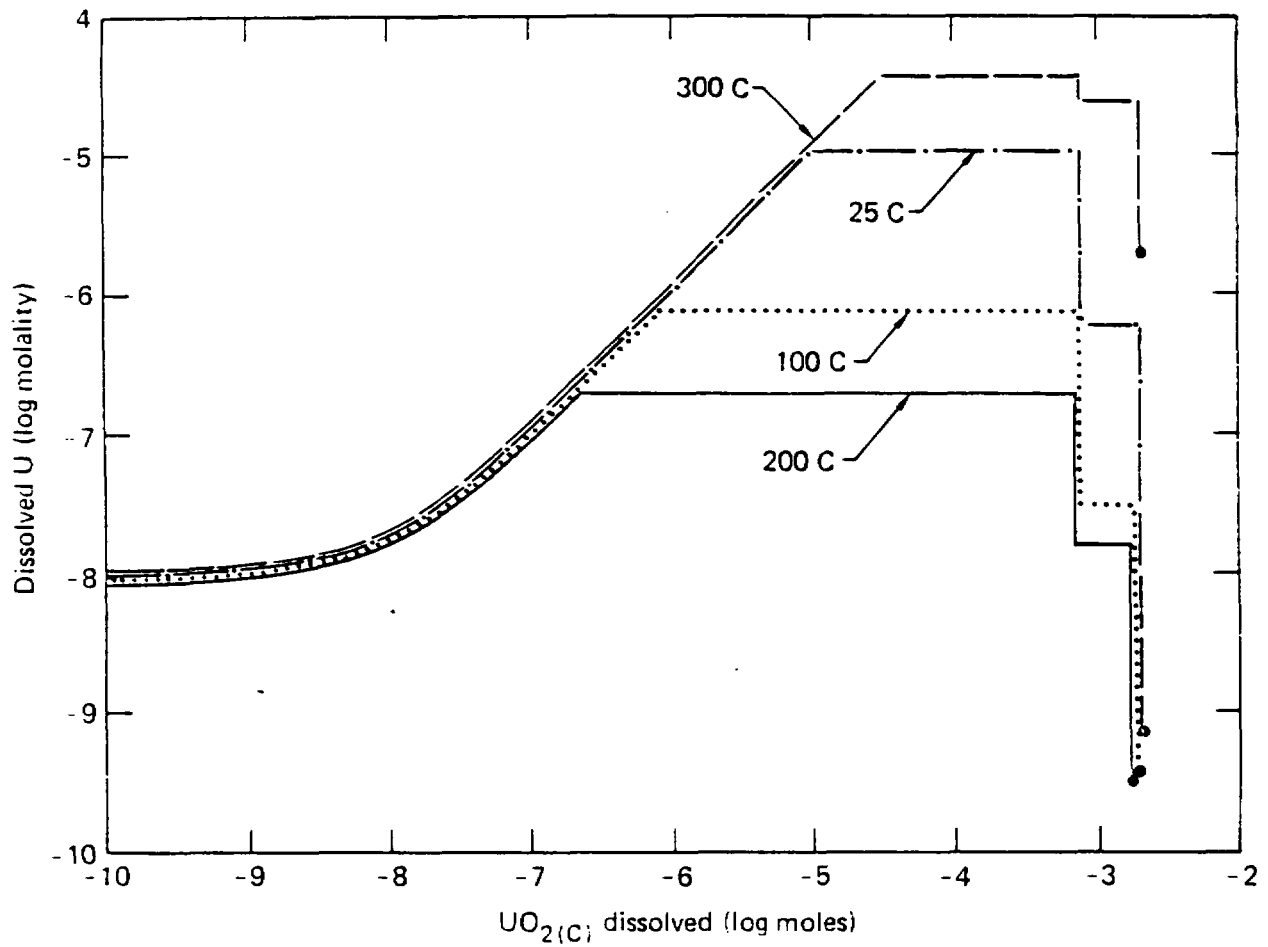
FIG. 7. Dissolved uranium produced by dissolution of $UO_{2(c)}$ in oxidizing granitic groundwater at 25, 100, 200, and 300 C. Some artistic license has been taken to separate the 100, 200, and 300 C curves from the 25 C curve and from each other.
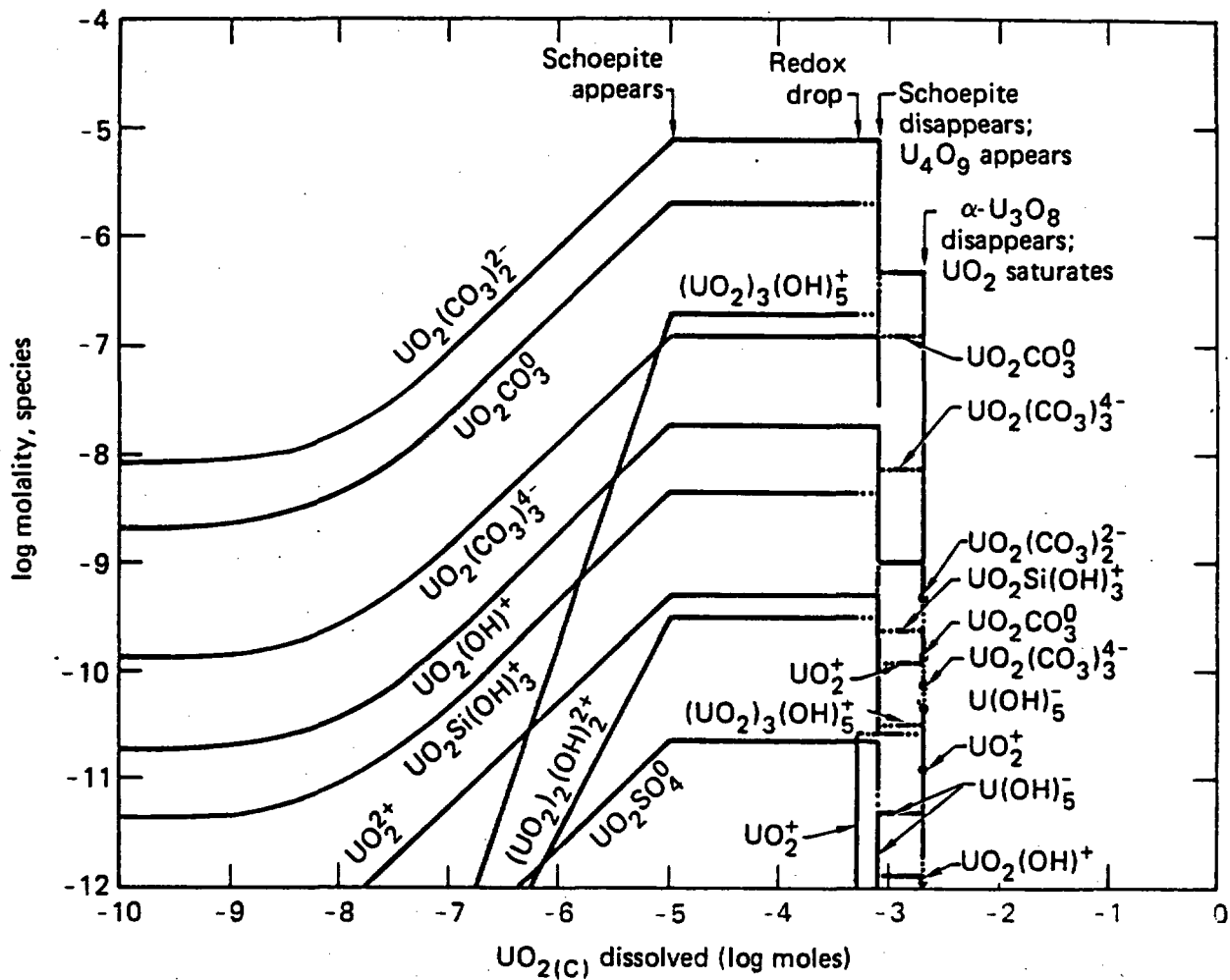
FIG. 8. Speciation of dissolved uranium produced by dissolution of $UO_{2(c)}$ in oxidizing granitic groundwater at 25 C.
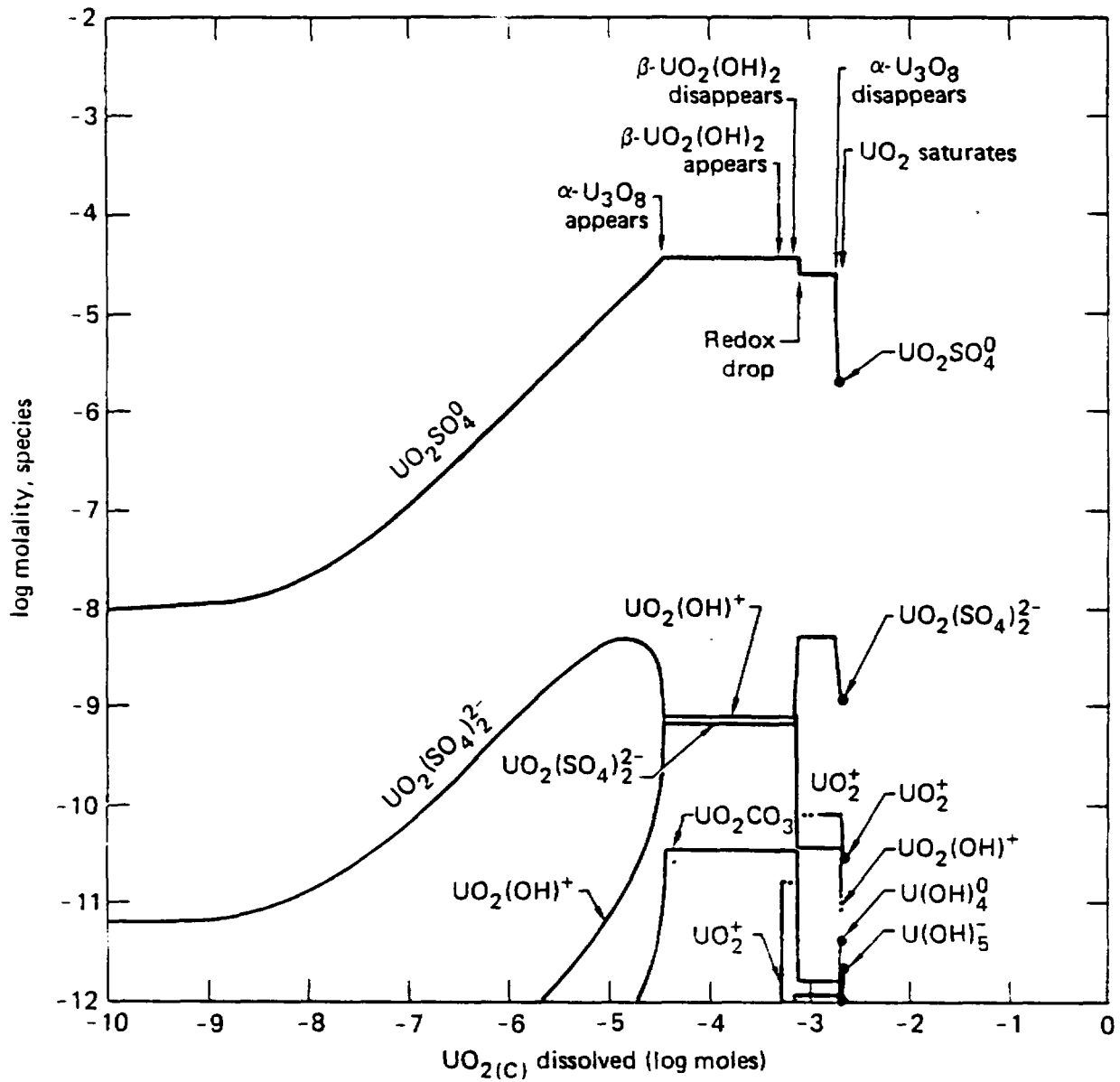
FIG. 9. Speciation of dissolved uranium produced by dissolution of $UO_{2(c)}$ in oxidizing granitic groundwater at 300 C.

The empirical temperature functions reported by Langmuir (1978) were used to extrapolate to 300 C.

The 300 C predictions may well be qualitatively correct. However, it seems clear that confidence in these predictions would be significantly enhanced by experimental measurement of the stability constants above 200 C of $UO_2SO_4^O$, $UO_2(SO_4)_2^{2-}$, and $UO_2(SO_4)_3^{4-}$, and also $U(OH)_3^+$, $U(OH)_4^O$, and $U(OH)_5^-$ (which may be more stable at 300 C than the extrapolations from 25 C predict). There are a few measurements of UO_2 solubility in pure aqueous and aqueous-electrolyte solutions at 400 and 500 C and 1 kilobar pressure which report high levels of dissolved uranium (Nguyen Trung and Poty, 1976), but the significance of these results to uranium chemistry at 300 C is not clear. At one point in the 300 C simulation, more than 99 percent of the dissolved sulfate was tied up in uranyl sulfate complexes. If there had been more dissolved sulfate to start with, or if the anhydrite $(CaSO_4)$ produced at 300 C by heating the groundwater from 25 C had been left in the system, the concentration of $UO_2(SO_4)_2^{2-}$ would not have begun decreasing due to swamping of dissolved SO_4^{-2} by UO_2^{2+} shortly after 10^{-5} moles of UO_2 had been dissolved (Fig. 9).

6.3 MODERATELY OXIDIZING GROUNDWATER

The major consequences of irreversible dissolution of UO_2 in moderately oxidizing granitic groundwater at 25 C are shown in Fig. 10. The basic patterns are very similar to those seen in the case of the oxidizing groundwater at the same temperature (Fig. 4), except for two main points. First, the scale on the abscissa has been expanded by a factor of over 100. This is a consequence of the fact that less UO_2 need dissolve in a solution initially containing less dissolved oxygen in order to reach saturation. The second major difference is that schoepite, $UO_2(OH)_2 \cdot H_2O$, does not appear as an alteration product. Consequently, there is no solubility limit on dissolved uranium prior to the redox drop at 2×10^{-6} mole UO_2 dissolved.

At 100 C, however, β-$UO_2(OH)_2$ appears (Fig. 11) in the same manner as before (Fig. 6). Similar consequences are manifested at 200 C. Once again, though, dissolved uranium behaves differently at 300 C than at 25, 100, and 200 C (Fig. 12). It increases to higher levels then at 100 and 200 C. At 300 C, however, no secondary precipitates formed--UO_2 simply dissolves congruently until the aqueous solution becomes saturated. Also, less UO_2 must dissolve to reach saturation at 300 C than at 25, 100, or 200 C.
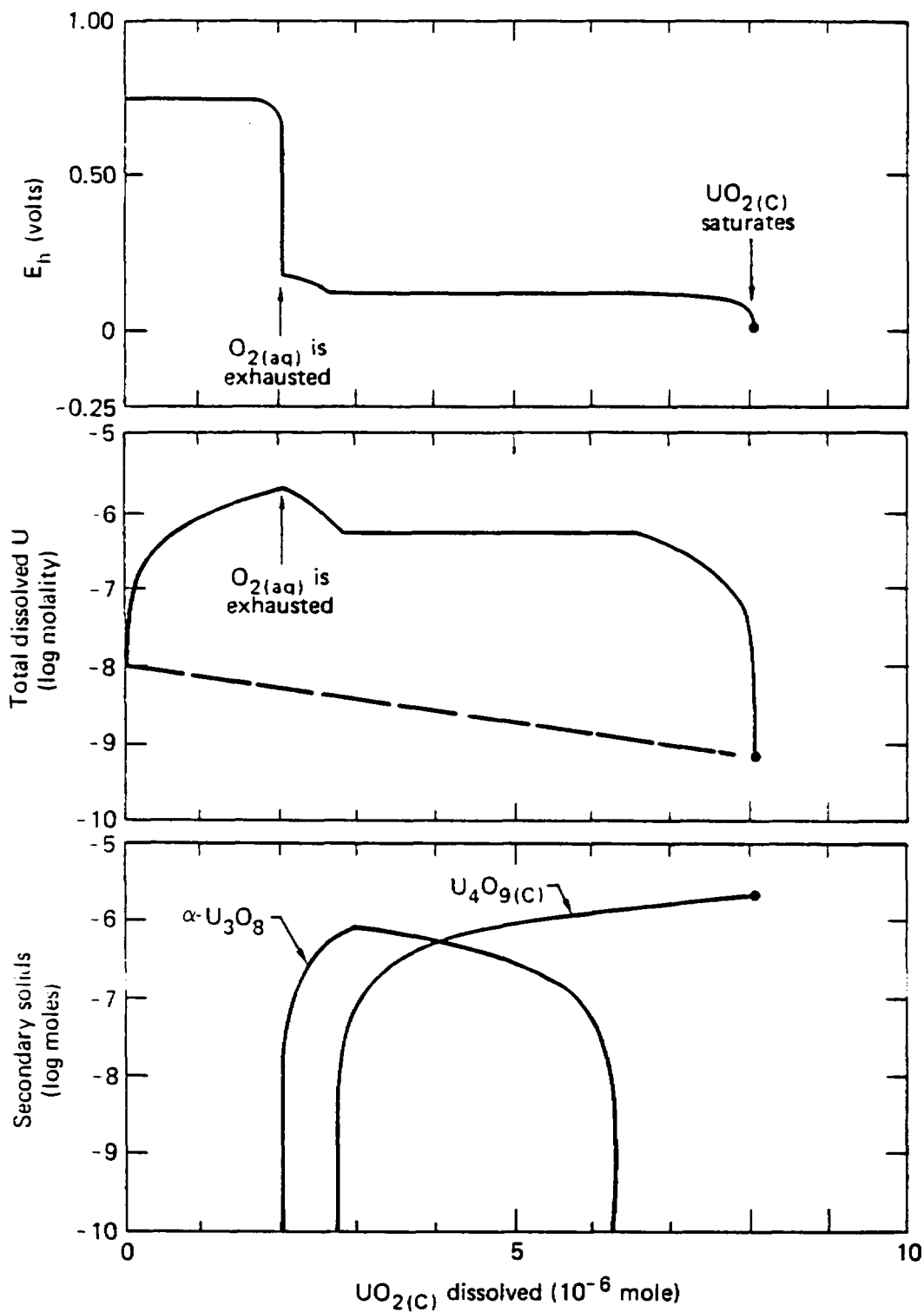
FIG. 10 Redox potential (E_h), dissolved uranium, and secondary solids produced by dissolution of $UO_{2(c)}$ in moderately oxidizing granitic groundwater at 25 C.

FIG. 11 Redox potential (E_h), dissolved uranium, and secondary solids produced by dissolution of $UO_{2(c)}$ in moderately oxidizing granitic groundwater at 100 C.

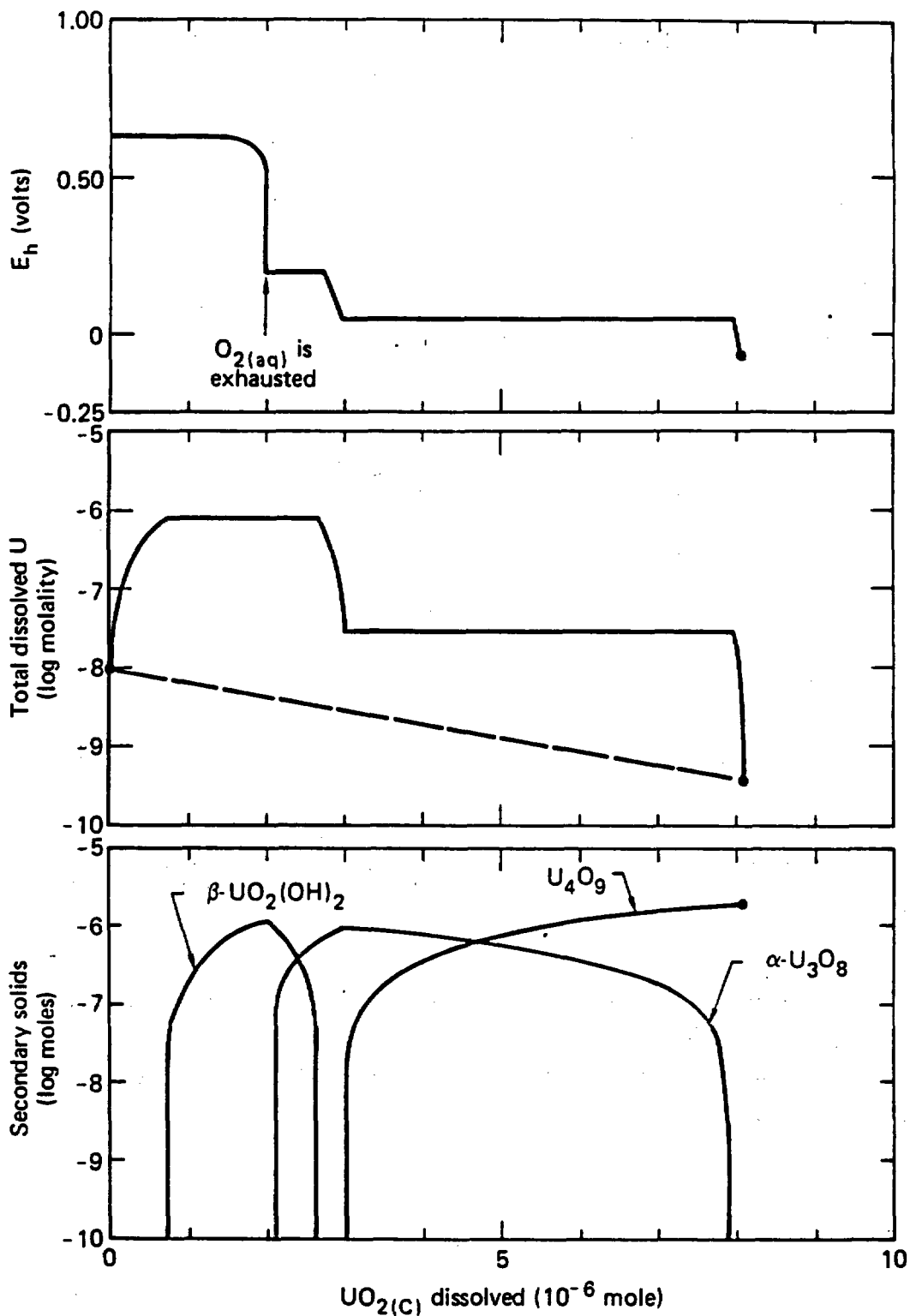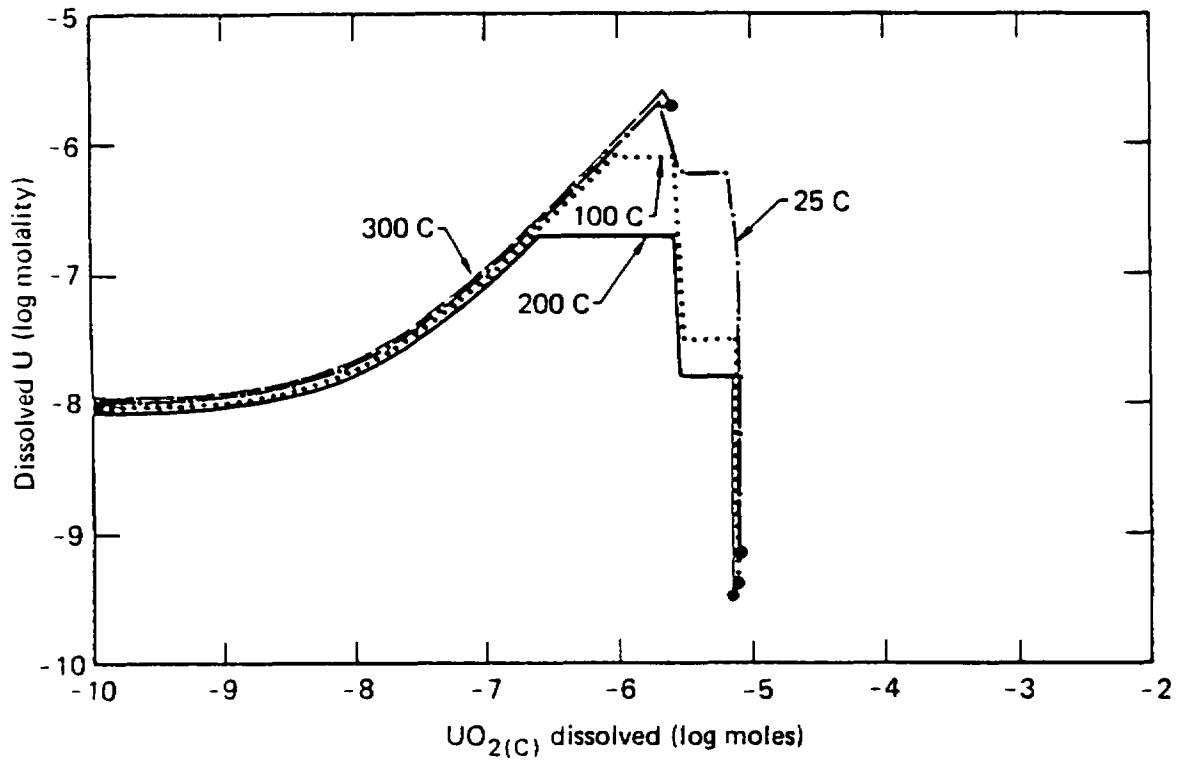FIG. 12. Dissolved uranium produced by dissolution of $UO_{2(c)}$ in moderately oxidizing granitic groundwater at 25, 100, 200, and 300 C. Some artistic license has been taken to separate the 100, 200, and 300 C curves from the 25 C curve and from each other.

6.4 REDUCED GROUNDWATER

The consequences of irreversible dissolution of UO_2 in the reduced granitic groundwater at 25 C are shown in Fig. 13. (Note the changes in scale). They are far less spectacular than those obtained for more oxidizing groundwaters. There was a much smaller change in the redox potential (Fig. 13, top). A miniscule transient increase in dissolved uranium occurred (Fig. 13, middle). The initial reduced solution was supersaturated with respect to cuprite $(Cu_2O_{(c)})$; a small amount of this mineral was precipitated prior to UO_2 dissolution. More of this phase formed in response to UO_2 dissolution (Fig. 13, bottom). It was later replaced by metallic copper, demonstrating the potential thermodynamic stability of this candidate waste packaging component in groundwater systems. No copper phases appeared in the higher temperature simulations, however.

The only secondary uranium phase to appear at 25 C was U_4O_9 (Fig. 13, bottom). At 300 C, no secondary uranium phases appeared, as was the case for the moderately oxidizing groundwater. Also, a significantly greater degree of dissolution and higher levels of dissolved uranium were again manifested (Fig. 14). The significance of the uranyl sulfate complexes was not diminished relative to other aqueous species bearing uranium.

6.5 CAVEATS

Several warnings are appropriate concerning the status and application of these simulations. These are given in part to facilitate intelligent comparison of such calculations with "real data." First, the simulations presented above pertain to closed systems of UO_2 plus aqueous solution. They do not pertain to closed systems of UO_2 plus aqueous solution plus air, or even UO_2 plus aqueous solution plus inert atmosphere. They especially do not apply to systems open to the atmosphere. However, our methodology does not exclude simulating such systems.

We have ignored any interactions between the system under study and container walls. Such interactions with laboratory vessels may occur by means of dissolution, sorption, or diffusion, and may pose difficulties in extrapolating laboratory data to field conditions. Again, our methodology does not exclude treating such phenomena in a modeling capability, but our

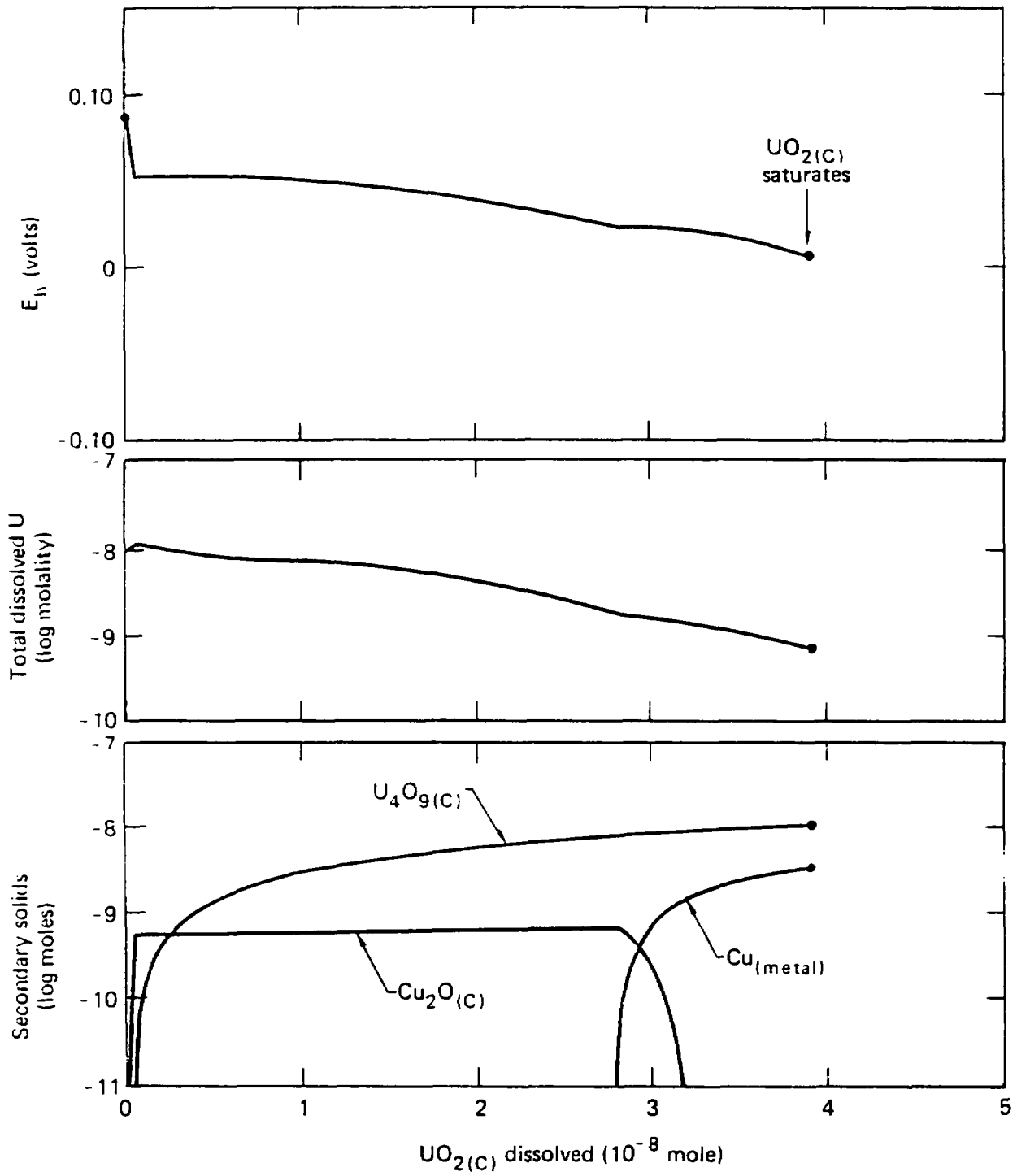FIG. 13. Redox potential (E_h), dissolved uranium, and secondary solids produced by dissolution of $UO_{2(c)}$ in reduced granitic groundwater at 25 C.
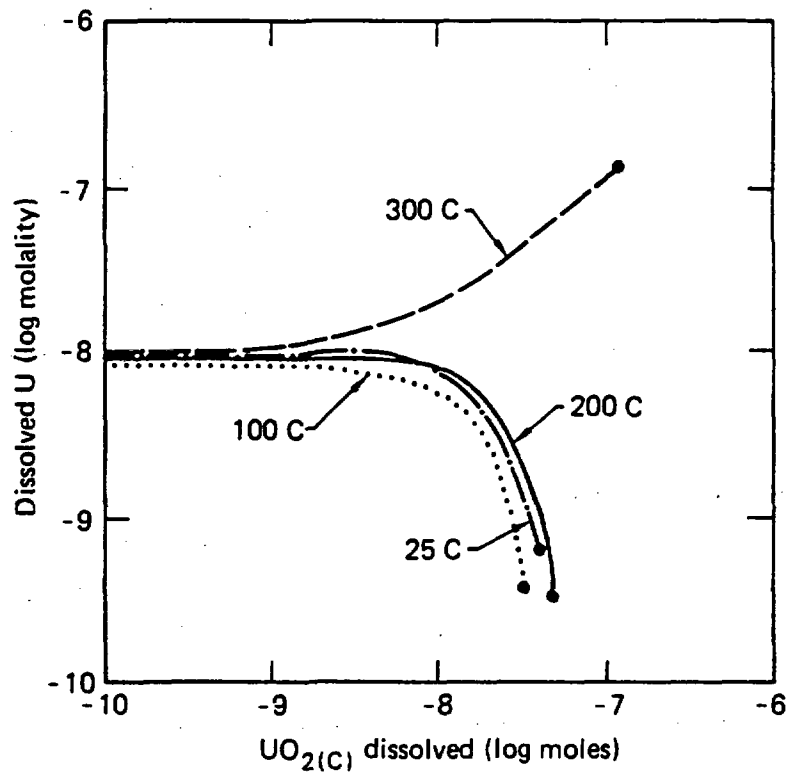
FIG. 14. Dissolved uranium produced by dissolution at $UO_{2(c)}$ in reduced granitic groundwater at 25, 100, 200, and 300 C. Some artistic license has been taken to separate the 100, 200, and 300 C curves from the 25 C curve and from each other.

software does not currently include provision for sorption, and diffusive mass transfer would require compartment-wise interfacing with another model.

Explicit treatment of irreversible dissolution kinetics must await further appropriate experimental measurements. Under oxidizing conditions at 25 C, UO_2 may dissolve at a rate of roughly 2×10^{-5} g/cm^2- day (Grandstaff, 1976). In the oxidizing region of our simulations of UO_2 dissolution in initially oxidizing and moderately oxidizing groundwaters the dissolution rate might be roughly constant at about this value. The time intervals corresponding to dissolution in these regions (Fig. 4, 0 to 5×10^{-4} mole UO_2 dissolved; Fig. 10, 0 to 2×10^{-6} mole UO_2 dissolved) would then be 67 and 0.27 days, respectively, assuming a contact surface area of 100 cm^2. In the region of low redox potential, we know of no meaningful experimental measurements of UO_2 dissolution. There is no basis to assume that the rates under oxidizing conditions also apply here.

The thermodynamic affinity of UO_2 dissolution, which from transition-state theory (Aagaard and Helgeson, 1977; Boudart, 1976; Lin et al., 1975) should influence the dissolution rate, does not vary in a simple manner with reaction progress. Figure 15 depicts this function for the simulation of UO_2 dissolution in the moderately oxidizing granitic groundwater at 25 C. In the oxidizing region (A $\approx$ 30 kcal), the affinity factor in Aagaard and Helgeson's rate law form is extremely close to the limiting value of unity, implying no rate dependence on affinity. In the reduced region (A $\approx$ 1.5 kcal), it has a value of 0.667, indicating a significant affinity dependence. We can not however, use these data to extrapolate rates measured under oxidizing conditions to reduced conditions without knowing the appropriate mechanism, which may not even be the same in both cases.

We have assumed that all the appropriate thermodynamic data were accurately represented in our simulations. This is probably true for the 25 C data. High-temperature data, however, are in large part obtained by extrapolation of 25 C data. Aside from the question of the accuracy of these extrapolations, one needs to consider the completeness of the high-temperature data. This is because 25 C data are generally complete and most accurate for the phases and aqueous species that are significant in 25 C systems. At high
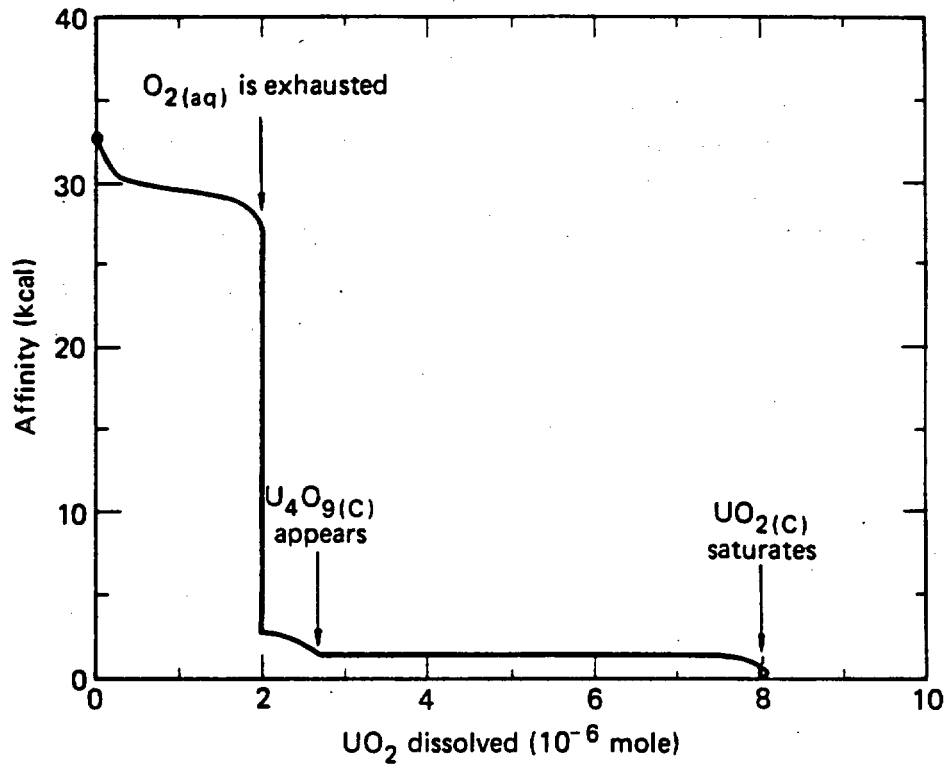
Fig. 15. Affinity of $UO_{2(c)}$ to dissolve during dissolution in moderately oxidizing granitic groundwater at 25 C.

temperature, the significant phases and species may include some not known or poorly studied at low temperature. Inaccuracies in thermodynamic data also propagate into calculated affinities, E_h, and pH, and hence into kinetic evaluations.

A caveat specific to the simulations presented here is that we have treated U_4O_9 and UO_2 as separate phases of fixed composition. In reality there is solid solution, apparently complete from UO_2 to $UO_{2.25}$ (a.k.a. U_4O_9; Langmuir, 1978). In a reaction-progress sense, this probably causes little difference (note: with the present software we could have treated this with a molecular mixing model given the appropriate excess Gibbs energy parameters; see Chapter 4). However, such solid solution may have a significant influence on the actual dissolution rates. In other words, the sequence of events and relative timing would probably change little, but the absolute timing might change considerably.

Chapter 7

MODELS OF UO_2/Cu METAL CODISSOLUTION IN
OXIDIZING GRANITIC GROUNDWATER

It is appropriate to include in this report some example of application
of the modeling methodology to a system more complex than UO_2-groundwater.
We have elected to present some simulations of UO_2-Cu codissolution in the
oxidizing granitic groundwater as an example of predicting interactions among
waste, packaging, and groundwater. These interactions may be stronger in the
near-field environment than those among waste, rock, and groundwater, because
metal containers may act as strong reducing agents. As oxygen getters, they
may protect the waste form to some extent even after they have been physically
breached.

Copper and its alloys have been proposed as packaging for nuclear waste
because they may be in or reach a state of equilibrium with invading
groundwaters (Ahlstrom, 1979). Stainless steel, among other metals, has also
been proposed for use in waste packaging. In contrast to copper and copper
alloys, it is thermodynamically unstable in geologic environments but may be
appreciably stable in a kinetic sense. Dissolution of small amounts of copper
packaging might occur quickly before equilibrium is reached, but no further
appreciable dissolution would occur without recharge of oxygenated
groundwaters. Normal deep groundwaters may contain little dissolved oxygen
and if so may be only slightly undersaturated with respect to copper metal or
its alloys.

Figure 16 shows the significant consequences of irreversible
codissolution of Cu and $UO_{2(c)}$ at 100 C. The relative rate of dissolution
is 100 to 1 (Cu to UO_2) and is fixed throughout the simulations until the
fluid becomes copper-saturated. The ratio of exposed surface areas would in
reality affect the relative dissolution rate. The contact area between a
metal and aqueous solution may decrease during oxidation due to the formation
of an oxide layer, whereas there is little evidence for the formation of
protective secondary products during dissolution of silicate minerals. (See
Chapter 3.) However, it is not probable that the relative rate of dissolution
would remain constant, even if the surface area ratio remained fixed. Note
that in this simulation, UO_2 dissolution commences with that of copper
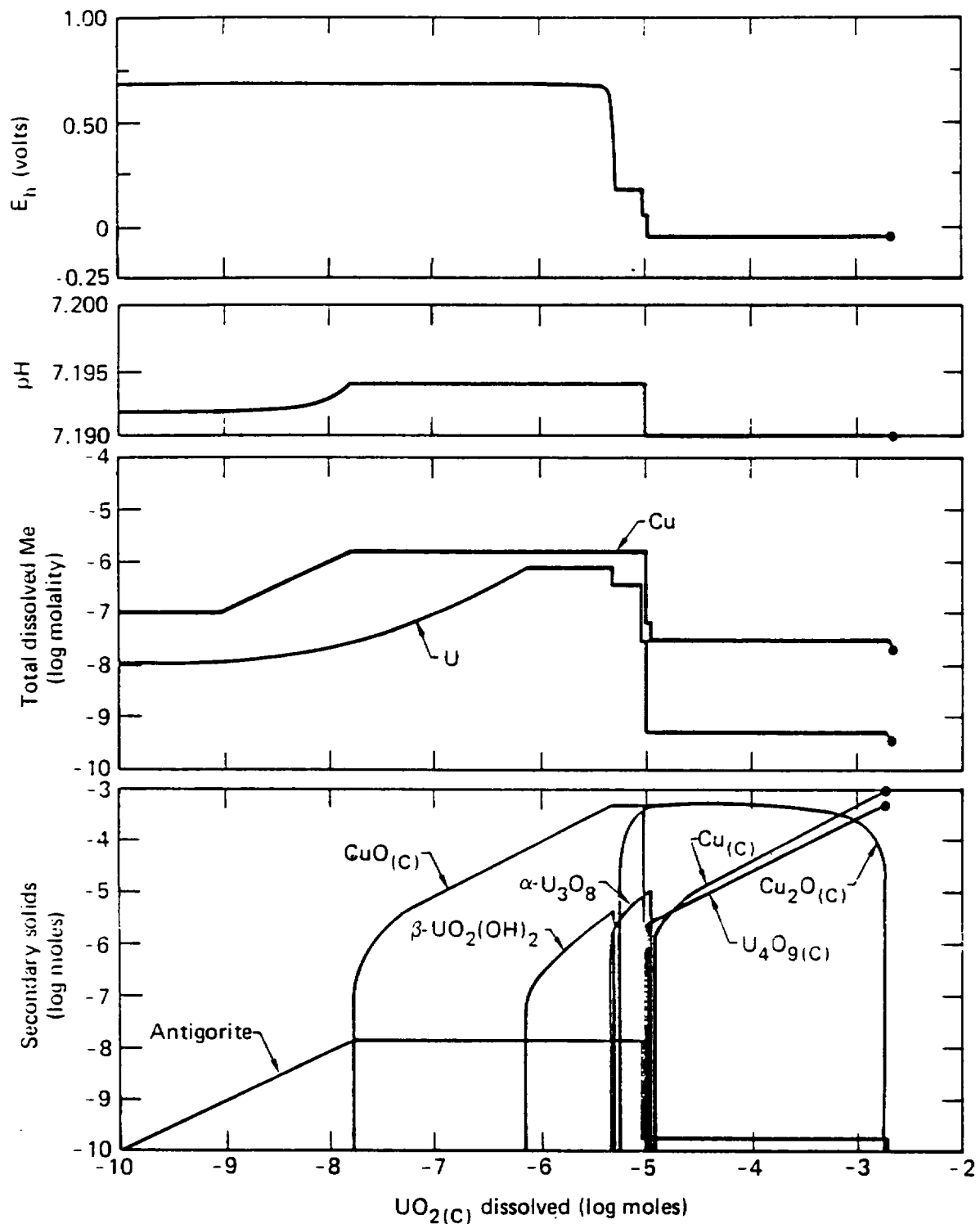
FIG. 16. Redox potential (E_h), pH, dissolved Cu and U, and secondary solids produced by co-dissolution of Cu metal and $UO_{2(c)}$ at relative rates of 100:1 at 100 C in oxidizing granitic groundwater. The $Cu_{(c)}$ plotted in the bottom of the figure represents only secondary (reprecipitated) metal.

(i.e., the container begins breached in this particular simulation). The modeling software could as easily have begun Cu dissolution prior to that of UO_2 (i.e., canister corrosion prior to breaching).

The redox potential (E_h, Fig. 16 top) drops in a manner similar to that seen previously in the simulations of UO_2 dissolution in oxidizing and moderately oxidizing groundwaters. Now, however, Cu competes with UO_2 for dissolved oxygen which is effectively exhausted more quickly. There are only very minor changes in the solution pH (Fig. 16 upper middle), though the trend closely parallels that of dissolved Cu (Fig. 16 lower middle). Both dissolved Cu and dissolved U exhibit transient high plateaus. Dissolved copper falls below the initial value near 10^{-5} mole UO_2 dissolved, where the fluid becomes saturated with pure copper. Irreversible dissolution of copper ceases while that of UO_2 continues until it also saturates near $10^{-2.7}$ mole UO_2 dissolved.

The secondary or alteration products include a very small amount of antigorite (a hydrous magnesium silicate) and sequences of copper and uranium minerals (Fig. 16, bottom). The secondary uranium mineral sequence is the same as that observed without copper codissolution at the same temperature (Fig. 6): $\beta-UO_2(OH)_2$, $\alpha-U_3O_8$, and U_4O_9. The secondary copper mineral sequence is tenorite (CuO) and cuprite (Cu_2O) followed by secondary copper metal. When the fluid saturates with respect to copper (at about 10^{-5} mole UO_2 dissolved) the original reactant copper ceases to dissolve. In response to the continued dissolution of UO_2, secondary copper is formed at the expense of cuprite and dissolved copper.

The results of a similar simulation (relative rate 100 to 1, Cu to UO_2, oxidizing granitic groundwater) at 300 C is depicted in Fig. 17. The drop in redox potential (E_h, Fig. 17 top) is similar but smoother. However, there is a more dramatic change in pH (Fig. 17, upper middle). Higher levels of both dissolved Cu and dissolved U are attained than at 100 C (Fig. 17, lower middle). The precipitation of antigorite is more significant (Fig. 17, bottom). Calcite ($CaCO_3$) also appears, but only transiently. U_4O_9 is the only secondary uranium mineral to appear. $\beta-UO_2(OH)_2$ and $\alpha-U_3O_8$ are absent although they appeared in the 100 C simulation discussed above and also in the 300 C simulation without Cu codissolution. Tenorite (CuO) does not appear in the sequence of secondary copper minerals in this 300 C simulation.

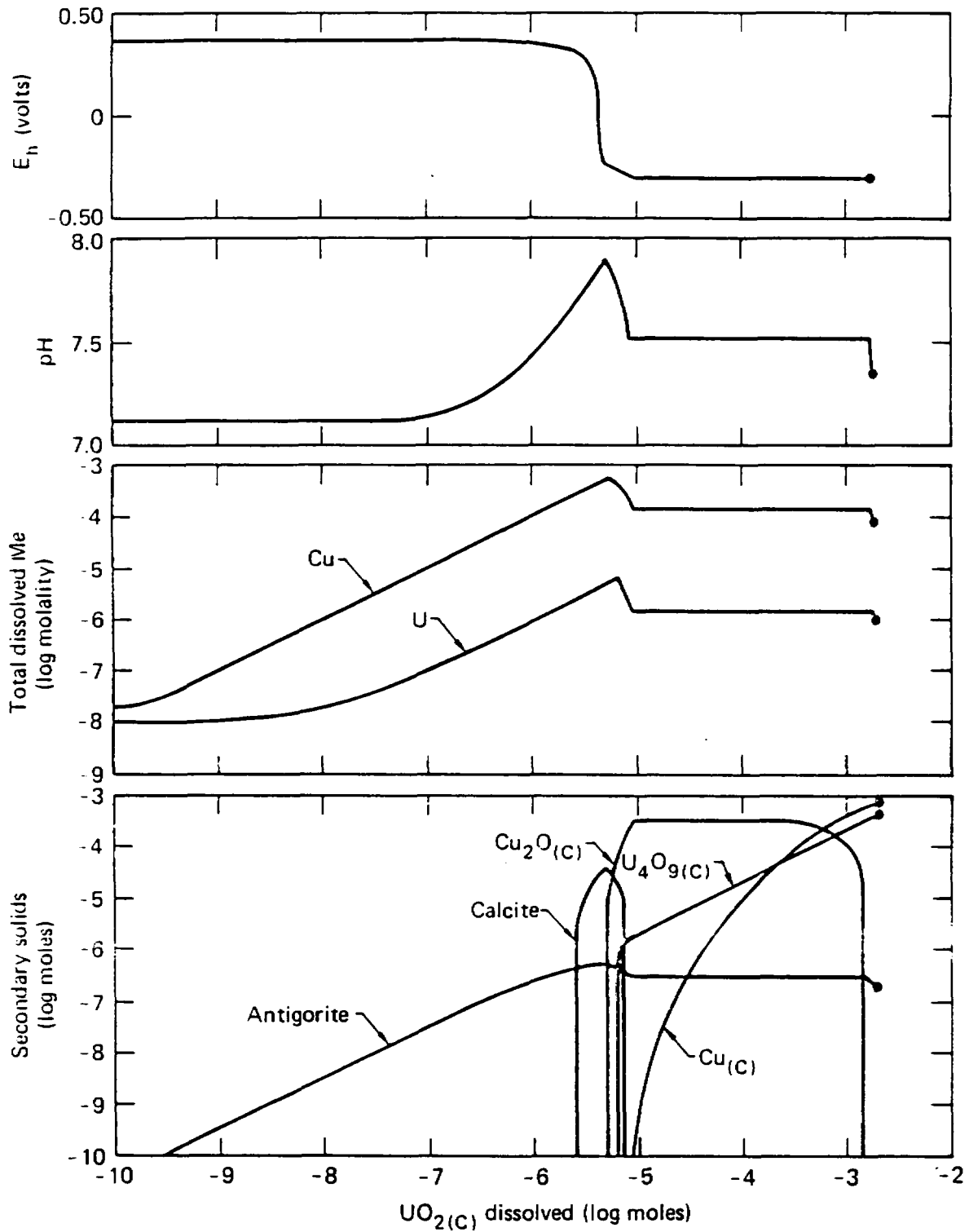FIG. 17. Redox potential (E_h), pH, dissolved Cu and U, and secondary solids produced by codissolution of Cu metal and $UO_{2(c)}$ at relative rates of 100 to 1 at 300 ℃ in oxidizing granitic groundwater. The $Cu_{(c)}$ plotted in the bottom of the figure represents only secondary (reprecipitated) metal.

Simulations of Cu-UO_2 codissolution of 100 C and 300 C were also done for relative rates of 10 to 1 and 1000 to 1 (Cu to UO_2). The dissolved uranium levels for the different relative rates of codissolution at 100 C are shown in Fig. 18. Increasing the relative rate of codissolution of Cu reduces the level of dissolved U more quickly, but the relative rate must approach 1000 to 1 to reduce the transient maximum value. This might also be achieved by a measure of irreversible dissolution of copper before initiation of irreversible dissolution of UO_2.

Figure 19 depicts the corresponding dissolved uranium results of 300 C simulations. At relative rates of Cu codissolution of 10 to 1 and greater, the maximum level of dissolved uranium is decreased.

The simulations presented in this report indicate that irreversible reaction of copper packaging with oxidizing groundwater may lead to a solubility equilibrium between packaging and groundwater and hence cessation of package deterioration due to chemical processes. This package-groundwater interaction may act to chemically ameliorate dissolution of UO_2. However, all the caveats discussed in the section on UO_2-groundwater simulations apply to these simulations also. Here, though, we see in addition the desirability of incorporating real kinetic rate laws into the model rather than having to assume arbitrary (and fixed) relative rates of irreversible co-dissolution. This point is also crucial to modeling similar scenarios involving rock, backfill, and chemical buffers.

FIG. 18. Dissolved uranium produced by codissolution of Cu metal and $UO_{2(c)}$ in oxidizing granitic groundwater at 100 C and relative rates of 0 to 1, 10 to 1, 100 to 1, and 1000 to 1. Squares mark saturation with respect to Cu metal. Some artistic license has been taken to separate the other curves from the 0 to 1 curve and from each other. All curves terminate at the same point (dark circle).
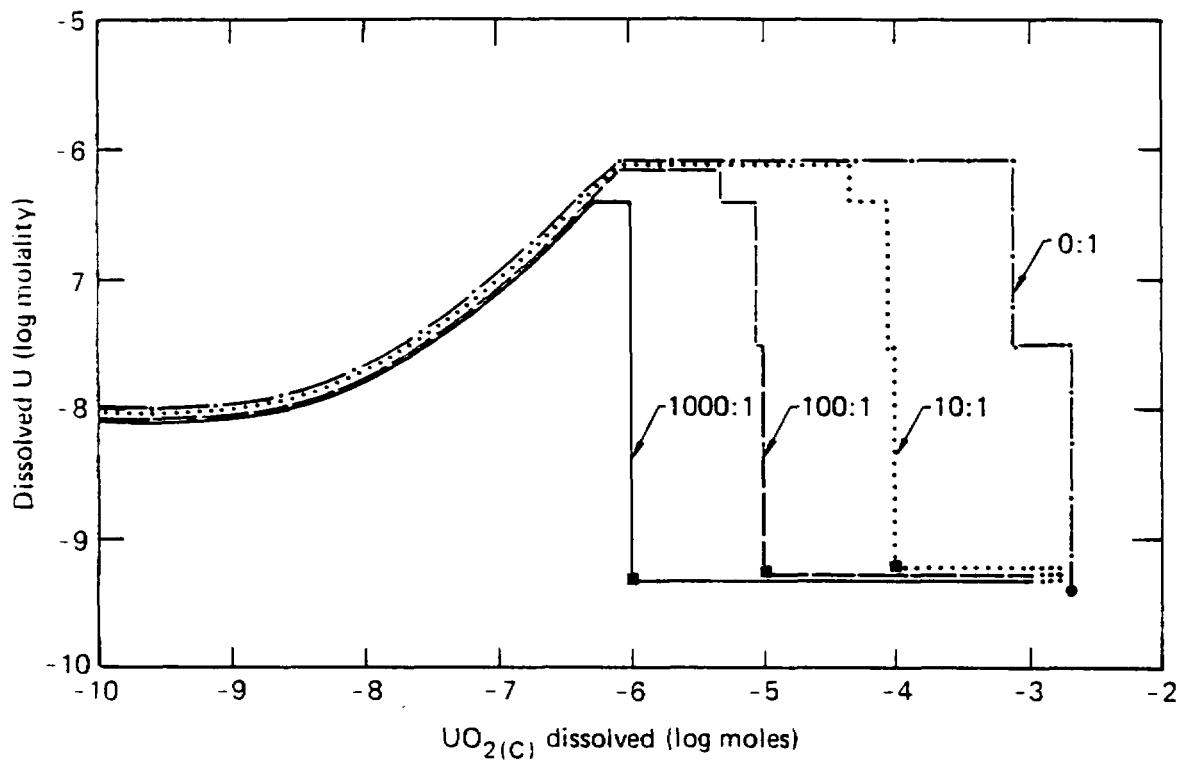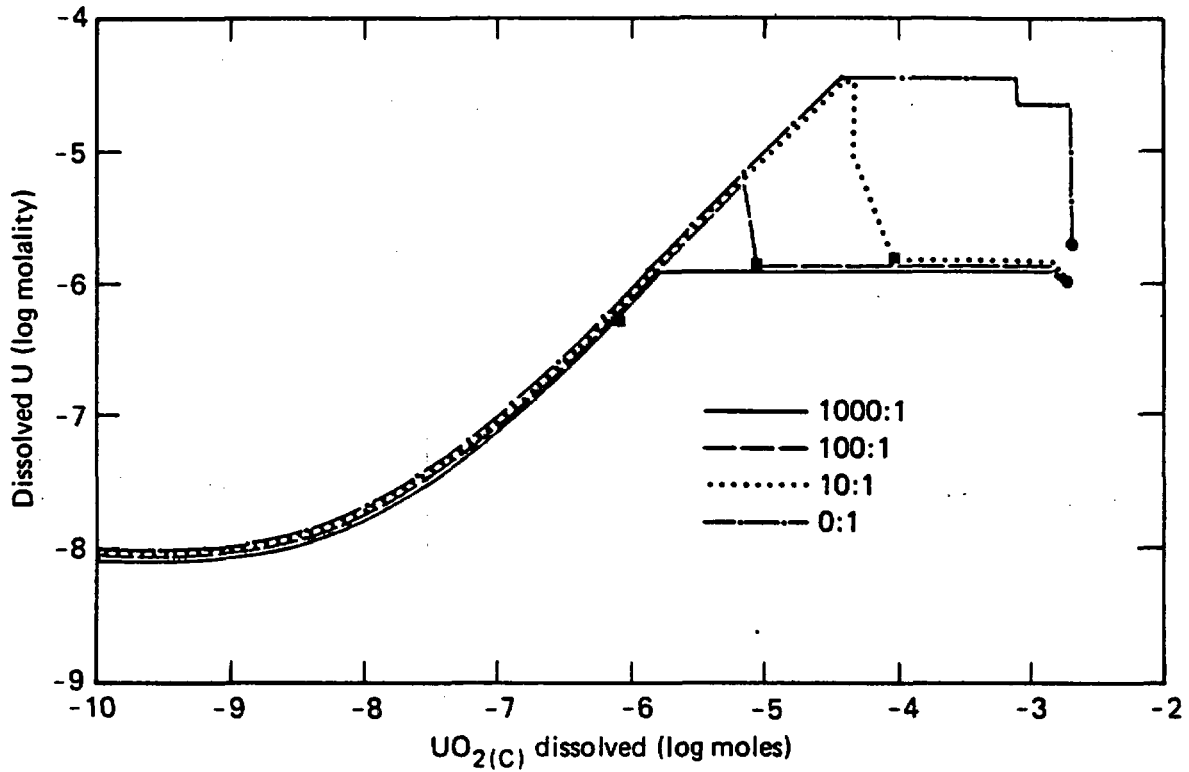
FIG. 19. Dissolved uranium produced by codissolution of Cu metal and $UO_{2(c)}$ in oxidizing granitic groundwater at 300 C and relative rates of 0 to 1, 10 to 1, 100 to 1, and 1000 to 1. Squares mark saturation with respect to Cu metal. Some artistic license has been taken to separate the other curves for the 0 to 1 curve and from each other.

REFERENCES

Aagaard, P., and Helgeson, H.C. 1977, Thermodynamic and kinetic constraints on the dissolution of feldspars, abstract, Geol. Soc. Amer. Abstracts with Programs. v. 9, p. 873.

Ahlstrom, P.-E., 1979, Ceramic and pure metal canisters in buffer material, p. 283-316 in L.A. Casey, ed., Proc. of the Conf. on High-Level Radioactive Solid Waste Forms. Dec. 19-21, 1978, Denver, Colorado. U.S. Nuclear Regulatory Commission, Office of Nuclear Material Safety and Safeguards, NUREG/CP-0005.

Apps, J. A., Benson, L.V., and Carnahan, C.L., 1978, Extension of experimental results with thermodynamic modeling: p. 145-149 in Basalt Waste Isolation Program Annual Report - Fiscal Year 1978, Rockwell Hanford Operations, Richland WA (RHO-BWI-78-100).

Barin, I., and Knacke, O., 1973, Thermochemical Properties of Inorganic Substances, Springer-Verlag, Berlin.

Barin, I., Knacke, O., and Kubaschewski, O., 1977, Thermochemical Properties of Inorganic Substances, Supplement, Springer-Verlag, Berlin.

Barner, H.E. and Scheuerman, R.V., 1978, Handbook of Thermochemical data for Compounds and Aqueous Species, John Wiley and Sons, New York.

Bell, M. J., 1973, ORIGEN - The ORNL Isotope and Depletion Code, ORNL-4628, Oak Ridge National Laboratory, Oak Ridge, Tennessee.

Berner, R.A., 1971, Principles of Chemical Sedimentology, McGraw-Hill Book Company, New York.

Berner, R.A., and Holdren, G.R., Jr., 1979, Mechanism of Feldspar weathering-II. Observations of feldspars from soils, Geochim. Cosmochim. Acta, v. 43, pp. 1173-1186.

Boudart, M., 1976, Consistency between kinetics and thermodynamics, J. Phys. Chem., v. 80, pp. 2869-2870.

Blander, M., 1972, Thermodynamic properties of orthopyroxenes and clinopyroxenes based on the ideal two-site model, Geochim. Cosmochim Acta, v. 36, pp. 787-799.

Brimhall, G. H., Jr., 1979, Theoretical confirmation of vein-forming mass transfer mechanisms of the porphyry copper environment: hypogene leaching and enrichment of protore, Geol. Soc. Amer. Abstracts with Programs, v. 11, p. 394.

Burkholder, H.C., 1979, Waste isolation performance assessment - a status report (ONWI-60), Office of Nuclear Waste Isolation, Battelle Memorial Institute, Columbus, Ohio.

Busenberg, E., and Clemency, C.V., 1976, The dissolution kinetics of feldspars at 25 C. and 1 atm CO_2 partial pressure, Geochim. Cosmochim. Acta., v. 40, pp. 41-49.

Criss, C.M., and Cobble, J.W., 1964a, The thermodynamic properties of high temperature aqueous solutions, IV. Entropies of the ions up to 200 C and the correspondence principle, J. Amer. Chem. Soc. v. 86, pp. 5385-5390.

Criss, C.M., and Cobble, J.W., 1964b, The thermodynamic properties of high temperature aqueous solutions. V. The calculation of ionic heat capacities up to 200 C. Entropies and heat capacities above 200 C, J. Amer. Chem. Soc., v. 86, pp. 5390-5393.

Davis, J.A., James, R.O., and Leckie, J.O., 1978, Surface ionization and complexation at oxide/water interface: 1. Computation of electrical double layer properties in simple electrolytes, J. Coll. Interface Sci., v. 63, pp. 480-499.

Freeze, R.A., and Cherry, J.A., 1979, Groundwater, Prentice-Hall, Inc., Englewood Cliffs, New Jersey.

Fritz, P., Reardon, E.J., and Barker, G., 1978, Carbon isotope geochemistry of a small groud water system in northeastern Ontario, Water Resources Research, v. 14, pp. 1059-1067.

Ganguly, J., 1977, Compositional variables and chemical equilibrium in metamorphism, pp. 250-284, in Saxena, S.K., and Bhattacharji, S., eds., Energetics of geological processes, Springer-Verlag, New York.

Garrels, R.M., and Christ, C.L., 1965, Solutions, Minerals and Equilibria, Freeman, Cooper, and Company, San Francisco.

Grandstaff, D.E., 1976, A kinetic study of the dissolution of uraninite, Econ. Geol. v. 71, pp. 1493-1506.

Helgeson, H.C., 1967, Thermodynamics of complex dissociation in aqueous solutions at elevated temperatures, J. Phys. Chem. v. 71, pp. 3121-3136.

Helgeson, H.C., 1968, Evaluation of irreversible reactions in geochemical processes involving minerals and aqueous solutions I. Thermodynamic relations, Geochim. Cosmochim. Acta. v. 32, pp. 853-857.

Helgeson, H.C., 1971, Kinetics of mass transfer among silicates and aqueous Solutions, Geochim. Cosmochim. Acta, v. 35, pp. 421-469.

Helgeson, H.C., Garrels, R.M., and Mackenzie, F.T., 1969, Evaluation of irreversible reactions in geochemical processes involving aqueous solutions II. Applications, Geochim. Cosmochim. Acta, v. 33, pp. 455-481.

Helgeson, H.C., Brown, T.H., Nigrini, A., and Jones, T.A., 1970, Calculation of mass transfer in geochemical processes involving aqueous solutions, Geochim. Cosmochim. Acta, v. 34, pp. 569-592.

Helgeson, H.C., and Kirkham, D.H., 1974a, Theoretical prediction of the thermodynamic behavior of aqueous electrolytes at high pressures and temperatures: I. Summary of the thermodynamic/electrostatic properties of the solvent, Amer. J. Sci., v. 274, pp. 1089-1198.

Helgeson, H.C., and Kirkham, D.H., 1974b, Theoretical prediction of the thermodynamic behavior of aqueous electrolytes at high pressures and temperatures: II. Debye-Huckel parameters for activity coefficients and relative partial-molal properties, Amer. J. Sci., v. 274, pp. 1199-1261.

Helgeson, H.C., and Kirkham, D.H., 1976, Theoretical prediction of the thermodynamic behavior of aqueous electrolytes at high pressures and temperatures: III. Equation of state for aqueous species at infinite dilution, Amer. J. Sci., v. 274, pp. 97-240.

Helgeson, H.C., Delaney, J.M., Nesbitt, H.W., and Bird, D.K., 1978, Summary and critique of the thermodynamic properties of rock-forming minerals, Amer. Jour. Sci., v. 278-A, p. 1-229.

Helgeson, H.C., and Aagaard, P., 1979, A retroactive clock for geochemical processes, abstract, Geol. Soc. Amer. Abstracts with Programs, v. 11, p. 442.

Hench, L.L., Clark, D.E., and Yen-Bower, E.L., 1979, Surface leaching of glasses and glass-ceramics, pp. 199-238 in Casey, L.A., ed., Proc. of the Conf. on High-Level Radioactive Solid Waste Forms, Dec. 19-21, 1978, Denver Colorado, U.S. Nuclear Regulatory Commission, Office of Nuclear Material Safety and Safeguards, NUREG/CP-0005.

Holdren, G.R., Jr., and Berner, R.A., 1979, Mechanism of feldspar weathering I. Experimental studies, Geochim. Cosmochim. Acta, v. 43, pp. 1161-1171.

Isaacson, R.E., and Brownell, L.E., 1973, Ultimate storage of radioactive wastes in terrestrial environments, pp. 953-986 in Symposium on the Management of Radioactive Wastes from Fuel Reprocessing, 27 Nov.-1 Dec. 1972, Organisation for Economic Co-operation and Development, Paris.

James, R.O., and MacNaughton, M.G., 1977, The adsorption of aqueous heavy
metals on inorganic minerals, Geochim. Cosmochin. Acta, v. 41,
pp. 1549-1555.

Kerrick, D.M., and Darken, L.S., 1975, Statistical thermodynamic models for
oxide and silicate solid solutions with applications to plagioclose,
Geochim. Cosmochim. Acta, v. 39, pp. 1431-1442.

Krauskopf, K.B., 1967, Introduction to Geochemistry, McGraw-Hill, New York.

Kubaschewski, O., and Alcock, C.B., 1979, Metallurgical Thermochemistry,
5th ed., Pergamon Press, Oxford.

Lagache, M., 1976, New data on the kinetics of the dissolution of alkali
feldspars at 200 C in CO_2 charged water, Geochim. Cosmochim. Acta,
v. 40, pp. 157-161.

Langmuir, D., 1978, Uranium solution-mineral equilibria at low temperatures
with applications to sedimentary ore deposits, Geochim. Cosmochim. Acta,
v. 42, pp. 547-569.

Lietzke, M. H., and R. W. Stoughton, 1960, The solubility of silver sulfate in
electrolyte solutions - VII. Solubility in uranyl sulfate solutions, J.
Phys. Chem., v. 64, pp. 816-820.

Lin, S.H., Li, K.P., and Eyring, H., 1975, Theory of reaction rates in
condensed phases, in Eyring, H., Yost, W., and Henderson, D., eds.,
Physical Chemistry: An Advanced Treatise, v. 7, pp. 1-56.

McCarthy, G.J., 1977, High-Level Waste Ceramics: Materials Considerations,
Nuclear Technol. v. 32, pp. 92-105.

Nguyen Trung, C., and Poty, B., 1976, Solubilite de UO_2 en milieu aqueux a
400 et 500°, et 1 kilobar, p. 37-39 in Rapport d' Activite 1976 Equipe
de Recherche sur les Equilibres entre Fluides et Mineraux, Centre de
Recherches Petrographiques et Geochimiques, Vandoeuvre-les-Nancy.

Nordstrom, D.K., Jenne, E.A., and Ball, J.W., 1979, Redox equilibria of iron
in acid mine waters, pp. 51-79, in Jenne, E.A., ed., Chemical Modeling in
Aqueous Systems, ACS Symp. Series 93, American Chemical Society,
Washington, D.C.

Nordstrom, D.K.; et al., 1979, A comparison of computerized chemical models for
equilibrium calculations in aqueous systems, pp. 857-892, in Jenne, E.A.,
ed., Chemical Modeling in Aqueous Systems, ACS Symp. Series 93, American
Chemical Society, Washington, D.C.

Oates, W.A., 1969, Ideal solutions, J. Chem. Educ., v. 46, pp. 501-504.

Paces, T., 1973, Steady-state kinetics and equilibrium between ground water and granitic rocks, Geochim. Cosmochim. Acta, v. 37, pp. 2641-2663.

Pelton, A.D., Schmalzried, H., and Sticher, J., 1979, Thermodynamics of $Mn_3O_4-Co_3O_4$, $Fe_3O_4-Mn_3O_4$, and $Fe_3O_4-Co_3O_4$ spinels by phase diagram analysis, Ber. Bunsenges. Phys. Chem., v. 83, pp. 241-252.

Petrovic, R., 1976, Rate control in feldspar dissolution-II. The protective effects of precipitates, Geochim. Cosmochim. Acta, v. 40, pp. 1509-1521.

Petrovic, R., Berner, R. A., and Goldhaber, M.B., 1976, Rate control in dissolution of alkali feldspars - I. Study of residual feldspar grains by x-ray photoelectron spectroscopy, Geochim, Cosmochim. Acta, v. 40, pp. 537-548.

Powell, R., 1978, Equilibrium Thermodynamics in Petrology, Harper and Row, New York.

Ringwood, A.E., 1978, Safe Disposal of High Level Nuclear Wastes: A New Strategy, Australian National University Press, Canberra, Australia.

Schwartz, F.W., and Domenico, P.A., 1973, Simulation of hydrochemical patterns in regional groundwater flow, Water Resources Research, v. 9, pp. 707-720.

Schwartz, F.W., and Smith, L., 1979, Modeling transport with geochemical reactions, abstract, Workshop on Geochemistry of Nuclear Waste Management, Pinawa, Manitoba, Canada, 4-5 Oct. 1979.

Sergeyeva, E.I., Nikitin, A.A., Khodakovskiy, I.L., and Naumov, G.B., 1972, Experimental investigation of equilibria in the system $UO_3-CO_2-H_2O$ in 25 - 200 C temperature interval, Geochem. Intl., v. 9, pp. 900-910.

Stoessell, R.K., 1979, A regular solution site-mixing model for illites, Geochim. Cosmochim. Acta, v. 43, pp. 1151-1159.

Stumm, W., and Morgan, J.J., 1970, Aquatic Chemistry, Wiley, New York.

Taylor, R.W., D.D. Jackson, T.J. Wolery, and J.A. Apps, 1978, Section 5: Geochemistry, p. 165-233 in Geothermal Resource and Reservoir Investigation of U.S. Bureau of Reclamation Leaseholds at East Mesa, Imperial Valley, California, LBL-7094, Lawrence Berkeley Laboratory, Berkeley, California.

Thorstenson, D.C., 1970, Equilibrium distribution of small organic molecules in natural waters, Geochim. Cosmochim. Acta, v. 34, pp. 745-770.

Ulbrich, H.H., and Waldbaum, D.R., 1976, Structural and other contributions to the third-law entropies of silicates, Geochim. Cosmochim. Acta, v. 40, pp. 1-24.

Villas, R.N., and Norton, D., 1977, Irreversible mass transfer between circulating hydrothermal fluids and the Mayflower Stock, Econ. Geol., v. 72, pp. 1471-1504.

Westall, J., and H. Hohl, 1980, A comparison of electrostatic models for the oxide/solution interface, Adv. Colloid and Interface Science, v. 12, p. 265-294.

White, D.E., Hem, J.D., and Waring, G.A., 1963, Chemical composition of subsurface waters, Chapter F in Fleischer, M., technical ed., Data of Geochemistry (sixth ed.) U.S. Geol. Surv. Prof. Pap. 440-F, U.S. Govt. Printing Office, Washington, D.C.

Wolery, T.J., Some chemical aspects of hydrothermal processes at mid-oceanic ridges-a theoretical study. I. Basalt-sea water reaction and chemical cycling between the oceanic crust and the oceans. II. Calculation of chemical equilibrium between aqueous solutions and minerals, Ph.D. thesis, Northwestern University, Evanston, Ill., 1978.

Wolery, T.J., 1979a, Calculation of chemical equilibrium between aqueous solutions and minerals: The EQ3/EQ6 software package, UCRL-52658, University of California, Lawrence Livermore Laboratory, Livermore, California.

Wolery, T.J. 1979b, Computer simulation of temperature-dependent equilibrium precipitation, Geothermal Resources Council, Transactions, v. 3, pp. 793-795.

Wollast, R., 1967, Kinetics of the alteration of K-feldspar in buffered solutions at low temperature, Geochim. Cosmochim. Acta, v. 31, pp. 635-648.

APPENDIX A

ERRATA TO UCRL-52658 (Wolery, 1979a)

I am indebted to Dr. Bruce Goodwin of the Whiteshell Nuclear Research Establishment (Atomic Energy of Canada, Ltd.) for bringing my attention to some errors in my earlier report (Wolery, 1979a).

p. 10, second equation (sample mass balance):
"s" subscripts should read "S"

p. 15, second equation (equivalent stoichiometric ionic strength):
"ν" should be "k"

p. 16, table 5, twelfth equation $(\partial \alpha_\epsilon / \partial \ell_{s \neq w})$:
"+" should be "-"

p. 16, table 5, twelfth equation $(\partial \alpha_z / \partial \log I)$:
after "$10^{\ell_{s}*}$" should be "$/\nu_{rs}$"

p. 18, table 6, first equation (C_w):
right-hand-side should be multiplied by "2.303 $\tilde{I}$"

p. 18, table 6, third and fourth equations (extended Debye-Hückel and power series):
right-hand-side should be multiplied by "2.303 I"

p. 18, table 6, footnote:
"∂I" should be "$\partial \log I$"
"$\partial \tilde{I}$" should be "$\partial \log \tilde{I}$"

None of these errors occurred in EQ6 programming except that on p. 18, table 6, first equation. This would have had a negligible effect on any EQ6 calculations. The activity of water is close to unity for electrolyte solutions whose ionic strength lies within the recommended range of the activity coefficient approximations (Wolery, 1979a, table 2). C_w under these conditions is close to zero. Even if calculations had been made for more concentrated electrolyte solutions, the effect of the error would only have been to slow down the rate of convergence in subroutine NEWTON.

In addition to the errors pointed out by Dr. Goodwin, I also discovered that "ξ" had been substituted for "ζ" throughout the report. "ξ" symbolizes the reaction progress variable, "ζ" was intended to symbolize reactant-tracking (or relative rate) coefficients. Corrections in the UCRL-52658 report should also therefore include:

p. 9, "ξ_1, ξ_2, ξ_3" should be ζ_1, ζ_2, ζ_3"

p. 25, eqn. (17) should be (also correcting sign errors)

$$-dn_\rho/d\xi \equiv \zeta_{1\rho} + \zeta_{2\rho}\xi + \zeta_{3\rho}\xi^2 \qquad (\rho = 1,\hat{\rho})$$

p. 25, eqn. (19) should be

$$n_\epsilon^t (\xi) = n_\epsilon^t (\xi=0) + \sum_{\rho=1}^{\hat{\rho}} k_{\epsilon\rho} (\zeta_{1\rho}\xi + \zeta_{2\rho}\xi^2/2 + \zeta_{3\rho}\xi^3/3)$$